Dynamic Model of Interactions between Orientation Selective Neurons in Primary Visual Cortex

Martin Andreev Asenov

4th Year Project Report
Artificial Intelligence and Computer Science
School of Informatics
University of Edinburgh

2016

Abstract

Our vision system is a complex machinery, able to convert the change in light we detect with our eyes, to meaningful objects, perception of depth and motion. The information undergoes multiple stages of transformations by different parts of our visual cortex. The primary visual cortex (V1) is responsible for one of the first stages of vision processing. One of its functions is edge detection, which is determined by group of interacting neurons. Some visual illusions are believed to be caused in that specific part of V1. It is important to understand those illusions as they can give us an insight to how neural computation is done.

In this report we explore a model of the orientation selective neurons in the primary visual cortex. Those neurons are responsible for detecting edges at different locations of what we see with our eyes. We have multiple neurons per location responding to different edge orientations. Their combined response forms our perception of the edge presented. Neurons for different locations are also connected to each other, influencing each other's responses. This can lead to change of the perceived orientations, leading to different visual illusions and effects. The connections between the neurons can be modeled using the elastica principle of smooth continuity - the smoother the curve connecting two neurons, the stronger they should be connected.

Existing work already explores a static model of those connections. However the effect, or modulation, of nearby neurons to a specific neuron is calculated only once, without the neuron influencing back its modulators. Moreover the modulation is calculated directly from the orientations presented, rather than mediated through the group of neurons responsible for that location. This report addresses both of those issues. We implement a dynamic model of the orientation selective neurons, with connections between different neurons defined by the elastica principle. We explore the differences between the dynamic and static model, to check if in a dynamic setting, we still experience the same effects. We find that in most cases the effect remains that same.

Acknowledgements

I want to thank my parents for their unconditional emotional and financial support during my studies. I want to thank my grandparents, uncles and aunts for being there for me too, supporting me and treating me like a celebrity every time I go back home.

I want to thank my supervisors for the long discussions and their very critical feedback. I learned a great deal about a field, that I had no previous knowledge in. I got an amazing and fun project to work on. I got a glimpse of what my life as a graduate student is going to be and I am looking forward to apply the knowledge I gained.

I want to say thank you to my friends, all those friends who feel like a family. You made my stay in Edinburgh the most amazing four years in my life. We pushed each other, we studied together, we had fun together, we shared an apartment together. We lived out of beer and popcorn during exam periods. We traveled the world. We pushed our limits. We were never afraid. And most importantly we had a story or two to tell to our grandchildren.

Finally I want to thank this person, who turned my life upside down. You made me feel, what I haven't felt before. It's been quite a journey and I am looking forward to see where this journey is going to end.

Table of Contents

Chapter 1

Introduction

In processing visual information, our brain seems to treat the greater whole as importantly as the individual details. This principle was explored by the Gestalt psychologists, whose work is often being summarized with Kofka's famous statement "The whole is *other* than the sum of the parts". There are various rules for grouping similar visual information. This includes, but not limited to, closely located objects, items with similar size or color, etc. Example of some of the rules can be seen in Fig.1.1.

- A: proximity
- B: similar color
- C: similar size
- D: common fate
- E: good continuation
- F: closure
- G: common region
- H: element connectedness

From S. Palmer, "Gestalt Perception", MIT Encyclopedia of Cognitive Science
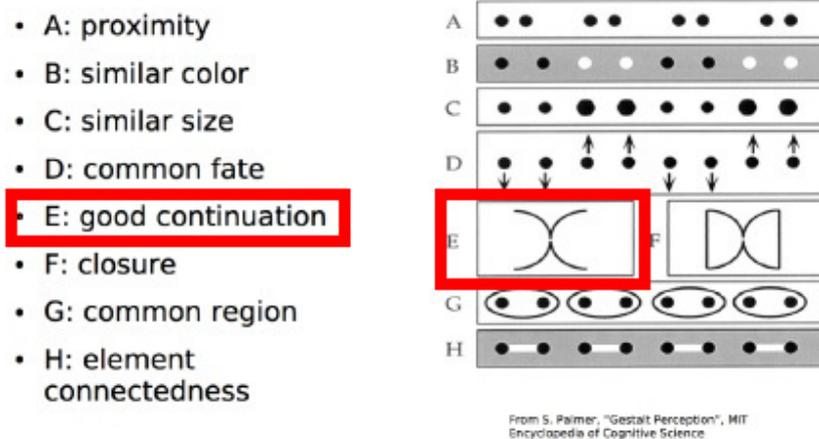
Figure 1.1: **Different groupings of Gestalt psychology.** Gestalt psychology specifies multiple rules for grouping objects, based on different criteria like proximity, similar color, etc. We are interested in the law of good continuation (highlighted in red). (Figure taken from [30])

The Gestalt psychology suggests the law of good continuation. According to this, humans tend to favour curves, bars, lines and edges with similar continuous direction. An example can be given even in he current words you are reading. The fact that they are all aligned, suggests the connectivity between them. More examples of good continuation are shown in Fig.1.2.
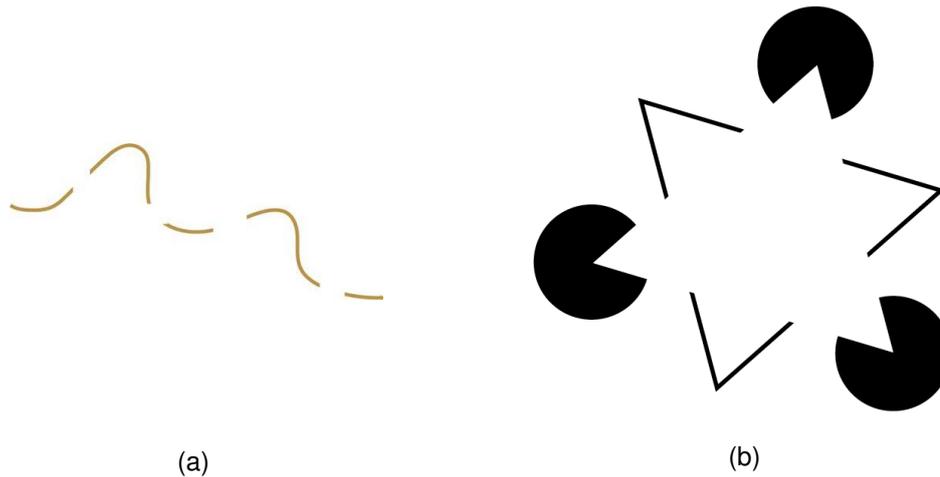
Figure 1.2: **Examples of good continuation.**   (a) Our brain promotes connectivity between the different segments presented, and we perceive them as one curve. (b) A more complex example of good continuation. Our brain interprets a white triangle at the top. If we look at individual parts of the image, nothing suggests that there should be one. However our brain assumes the different parts are just continuations of the same object. (figures taken from [28] [18])

The law of good continuation, seems to be implemented at the earliest stages of our visual pipeline, with evidence pointing to the primary visual cortex(V1) [7]. V1 is responsible for low-level edge detection. At each visual location neurons are tuned for different orientations. This 'stack' of neurons, responsible for a particular location, gives us a perception of the bar presented at that location. However, it is also known that neurons at different locations can also influence each other, rather than acting independently. Those interaction follow the law of good continuation, which has lead to the development of "association fields" models [7]. Association fields are governed by the rules of smooth curves, where the smoother the curve between two bars, the stronger they should be connected. The principle is illustrated in Fig.1.3.
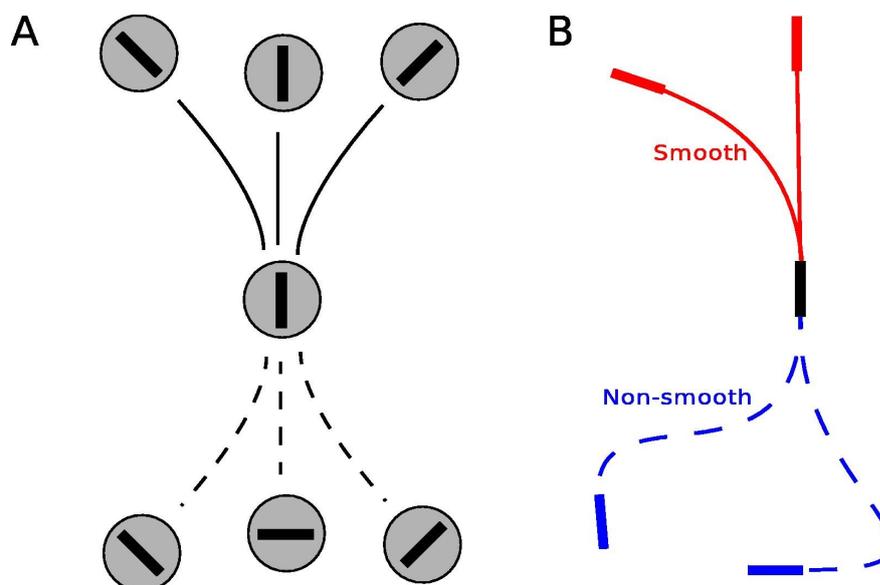
Figure 1.3: **Association fields.** a) Solid lines represent stronger connections, doted lines - weaker. b) Relation to smooth continuation. (Figure taken from [16])

The smoothest curve connecting two bars can be described by the elastica principle (latin for 'thin strip of elastic material' [20]). Elastica has a long history dating back to 13th century [20]. Jordanus de Nemore posed the problem, but provided an incorrect solution. A couple of centuries later the necessary mathematical techniques were developed. The first solution was published by James Bernoulli in 1694. The theory behind elastica is the base for designing mechanical splines, which are widely used in shipbuilding 1.4. Moreover, elastica has many analogies with different systems, like a sheet holding volume of water or the surface of a capillary [20].

The elastica energy quantitatively measures how strongly two bars are connected. Given their orientations and locations, the energy is defined as the total curvature of the smoothest curve connecting them. The smoother the curve is, the more strongly they should be connected. We use this energy to specify the strength of the modulation between orientation selective neurons.
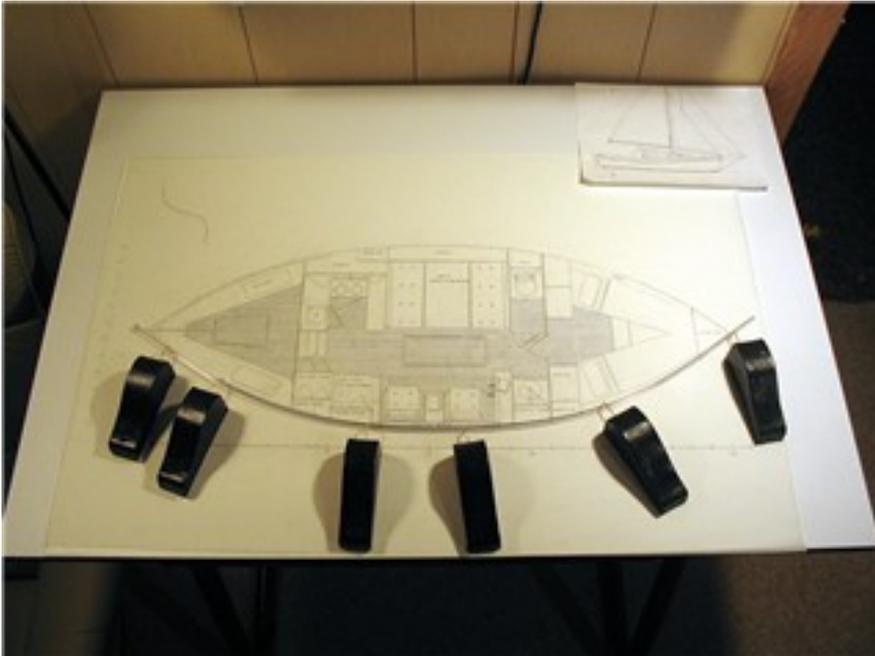
Figure 1.4: **Elastica in mechanical splines and shipbuilding.**   Elastica is the mathematical model behind mechanical splines [20]. One of the applications of mechanical splines is in shipbuilding . In this example the mechanical spline is used for designing the hull of an sailing vessel. (Figure taken from [27])

Incorporating the elastica principle for modelling interactions between orientation selective neurons have been shown to explain number of visual effects [16]. The model reproduces some tilt illusions, where the perceived orientation of a bar is different from the presented orientation, based on the orientation of nearby ones (Fig.1.5). Elastica also justifies some pop out effects, where we can detect unique bar among others with the same orientation. Finally it also explains contour extraction.
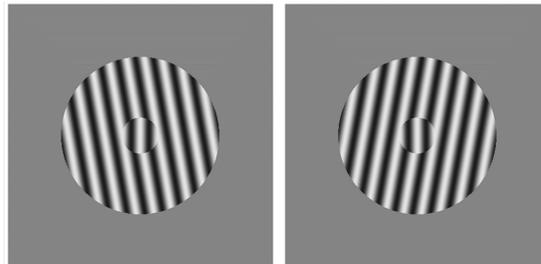
Figure 1.5: **Example of tilt illusion.**   The center circles seem tilted to each other, although in reality they are not. The effect is caused by the modulation from the bigger circles, around the center ones. (Figure taken from [3])

All the results in [16] were obtained by neurons getting a input based on the orientations in an image. We extend the model so neurons are directly connected to each other. Moreover the modulation between the neurons in [16] is calculated only once. The details of the illusions, pop out effects and contour extraction described in [16]

might depend on the static nature of the original model, and it is crucial that we understand how they come to be in a dynamical mode. We build a recurrent neural network of the orientation selective neurons in the V1 cortex, with modulation between them based on the elastica principle. We reproduce the experiments from the static model in [16] and compare the results in full dynamic setting, in the context of biological evidences for different illusions.

Different parts of the problem and work conducted are discussed in the report.

Background - gives some necessary neuroscience background and information about the problem. We talk about different concepts why they are relevant to the project and how we are going to use them.

Design - discuss the design of the experiments and the evolution of the model, before the final version used for running experiments.

Implementation - choice of programming languages and libraries, why they are important to the project and how they influence both the speed and ease of running experiments, but also the workflow of conducting research.

Experiments - in depth description of experiments ran

Evaluation - comparing the results gathered from experiments

Timeline - timeline of the work done through the project.

Conclusions - final conclusions

Chapter 2

Background

In explaining the model setup and performed experiments, it is important to first introduce some neuroscience terminology. As one can imagine the visual cortex is utterly complex. We are focusing on the V1 cortex, analyzing a specific type of orientation selective neurons. We describe the concepts of visual field, receptive fields, tuning curves and population coding. This chapter aims to give a brief introduction to the used terminology, before we fully explain our model in the Sec.3 of the report.

2.1 Visual field

Visual field is the area we can see with our eyes. The information undergo a variety of transformations in the different parts of our visual cortex. The first few processing steps are illustrated in Fig.2.1. The initial information we receive is changes in light from our retina. This then gets processed by the lateral geniculate nucleus (LGN). The LGN cells passes down the signals to the primary visual cortex (V1). V1 extracts information about edges and orientations in the different parts of our visual field.
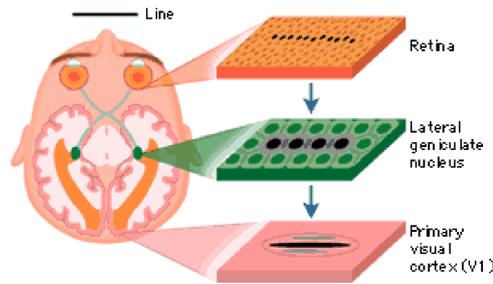
Figure 2.1: **Representation of a line in the primary visual cortex.** Here we display the first few layers of our vision system - retina, LGN cells and primary visual cortex. The retina and LGN cells do the initial vision processing. The primary visual cortex is responsible for edge detection at different part of our visual field. (Figure taken from [23])

Precisely how this information is processed is the main interest of this project. While at the retinal and LGN level, most of the transformations are local, V1 starts to extract some patterns. We don't only detect single orientations for different parts of our visual field. Closely located bars with similar angles can influence each other. These extracted patterns are useful for the high level visual processing happening in V2, V3, V4, V5 and V6.

Finally, it is also worth mentioning that we see in different details depending on position on visual field. More neural activity is dedicated to foveal (central vision) than ourside fovea, which could lead to interesting behavior [17]. A small part of our retina, known as 'blind spot', does not have any photoreceptors. Our brain compensates the lack of information by fulfill in details from nearby observations. Both of those details could change behavior in our model, however we will ignore this details in our experiments. Our retina and its associated neurons also suggest interactions between closely located bars and edges (Fig.2.2).
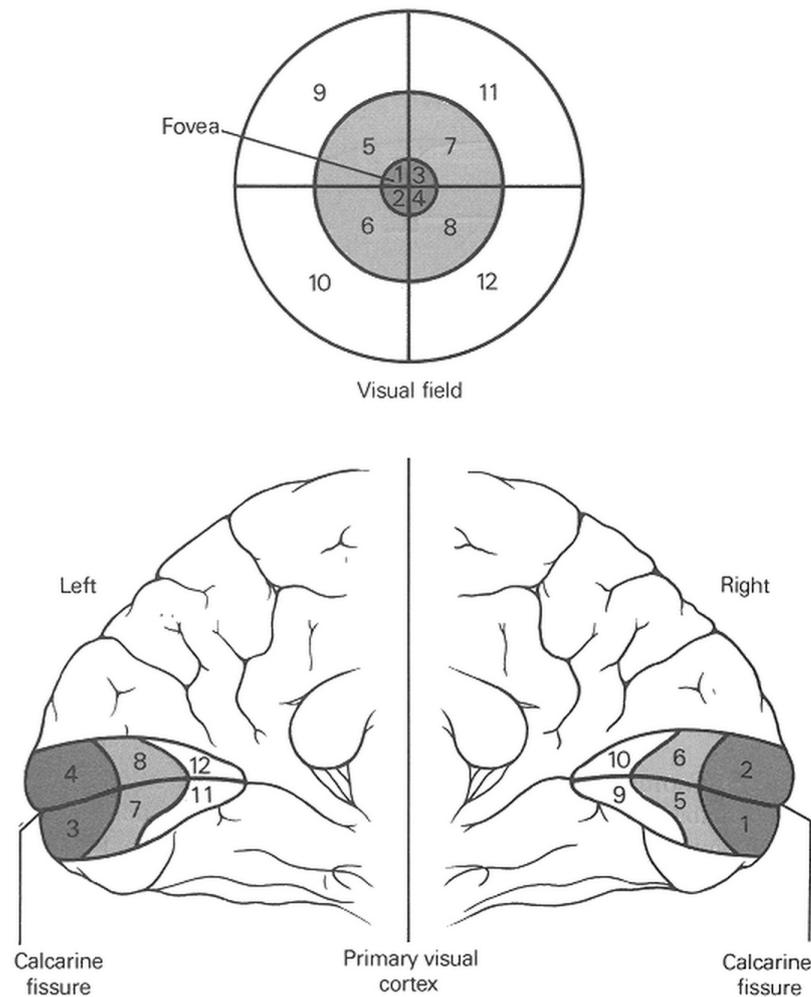
Figure 2.2: **Retinotopy.** Retinotopy is mapping retinal inputs to neurons. In the figure we have the retina at the top and the neurons corresponding to the different parts of the retina at the bottom. Substantial number of the cells in the retina are devoted to only a small part of our visual field, or central vision. Although relevant to the project, we will ignore this detail, for the benefit of simpler model. We notice that the mapping from the retina to neurons preserves their relative position. For example sector 3 and 4 are closely located in the retina, and the neurons responsible for them as closely located in the brain. This align with our theory that closely located bars and edges in our visual field can influence each other. (Figure taken from [5])

2.2 Receptive fields

In general, a receptive field is defined as a region of the sensory space, which can stimulate a given sensory neuron. In our context we can define the receptive field of a neuron, as the part of visual field, which affects it [10]. The above two definitions are known as classical receptive fields.

It was later discovered that time plays a role as well, making the definition more complicated [6]. In our model, described later, we focus on the spatial and ignore the temporal separation of receptive fields. Moreover because neurons are connected to each other, the notion of receptive field can get a bit vague. Because of those connections a neuron, can get excited or inhibited from parts of the visual field, that the neuron is not directly connected to.

To avoid confusion we will distinguish between the input a neuron receives because of its tuned orientation and modulation from nearby neurons. The classical receptive stimulus leads to response. The extra-classical receptive field modulates that response but causes no response by itself (Fig.2.3).
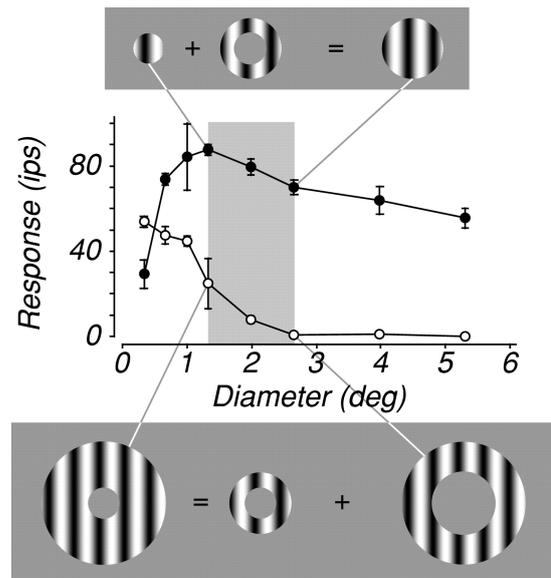

Figure 2.3: **Effect of the context on receptive field on a neuron.** The firing of neurons is indirectly modulated and their response shifted, based on the stimuli just outside of their receptive field. This leads to some of the complications of explaining receptive field. Even though a certain neuron is tuned for only a certain part of our vision field, for certain orientation, it can be affected by nearby neurons. If we take this to the extreme, then a receptive field is based on all the sensory input we receive, since one neuron excites a nearby one, which excites its nearby neurons, etc. (Figure taken from [4])

2.3 Tuning curves

Orientation selective neurons are tuned for different orientation at a specific part of the visual field, defined by their receptive field. In other words neurons like specific orientation at a specific place. However they spike not only when the preferred orientation is presented, but also when similar to its preferred orientation are. The intensity of spiking, when different orientations are presented, forms a bell shaped curve with a peak the preferred orientation of the neuron (Fig.2.4).
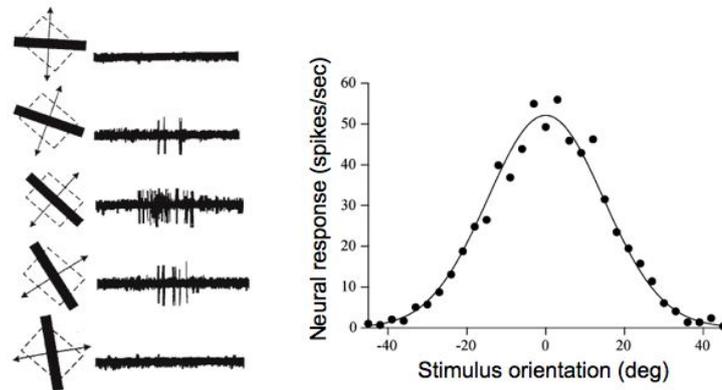
Figure 2.4: **Tuning curves.** Different orientation bars are presented in a certain part of the visual field (on the left), and the response of the neuron tuned for this specific part of the visual field and $0°$ (on the right). Even though the neuron is tuned for $0°$, it spikes when similar orientations are presented. The closer the orientation is to its preferred one, the stronger the response. (Figure taken from [11])

2.4 Population coding

We have multiple orientation selective neurons for a single location of our visual field. They all spike with different intensities based on their preferred orientation and bar presented. We assume that the perceived orientation is calculated by vector addition as described in [2] [8] [9] [16]. We can represent the spike of every neuron as a vector. The direction of the vector is the preferred orientation of the neuron. The length of the vector is the magnitude of the spiking. By adding all the vectors together we get a new vector, representing the perceived orientation. Similarly, the direction of the vector is the perceived orientation and the length is the magnitude of the response (Fig.2.4).
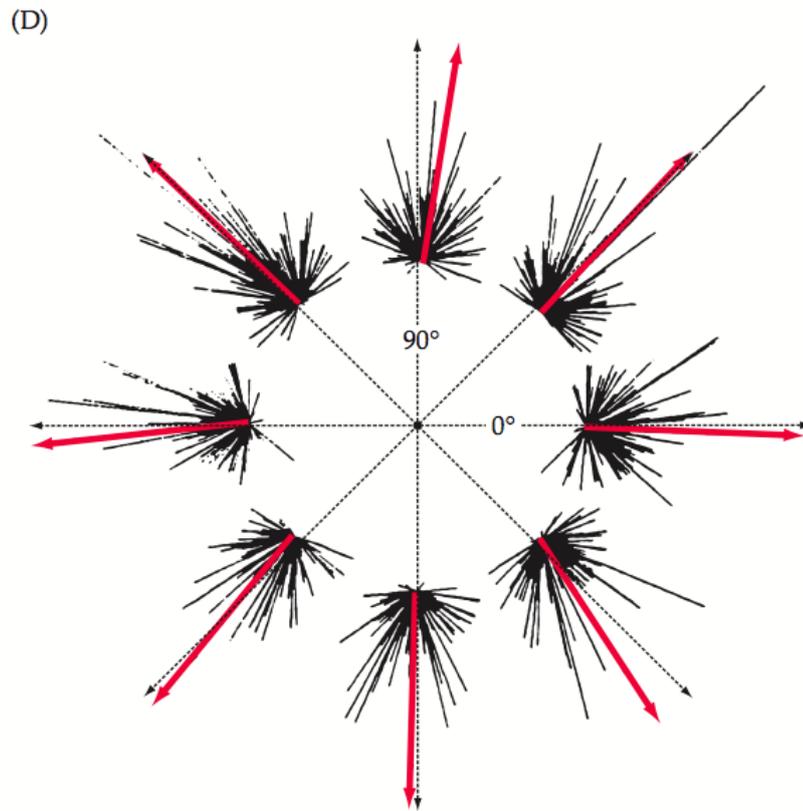
(D)

Figure 2.5: **Population coding in the motor cortex.**   Although the above picture illustrates population coding in a different part of the brain, it is still a good illustration of population coding. Orientation selective neurons respond with certain intensity (black bars). Their responses are combined to show the final perceived perception(red bars). (Figure taken from [1])

Chapter 3

Design

This report implemented versions of visual field, receptive fields, tuning curves and population coding. We simulated the primary visual cortex in a recurrent neural network. We started with a simple model with one receptive field. We extended the model to multiple receptive fields, defined limited and full connectivity. Finally, we implemented the elastica principle as well. In this section the different models are described in detail. In designing the model, we decided to use iterative and incremental development. The initial models were mostly used for validity checks, rather than any meaningful experiments. Most of our experiments were based on the final version of the model, with full connectivity with weights setup according to the elastica principle.

3.1 Overview

Our model receives as input a field of orientation bars. It outputs the perceived orientations and the overall activity of the neurons. As our our model is dynamic is changes with respect to time, we get this data for every time step of the simulation. An example input and output (for the stable state of the network) can be seen in Fig.3.1.
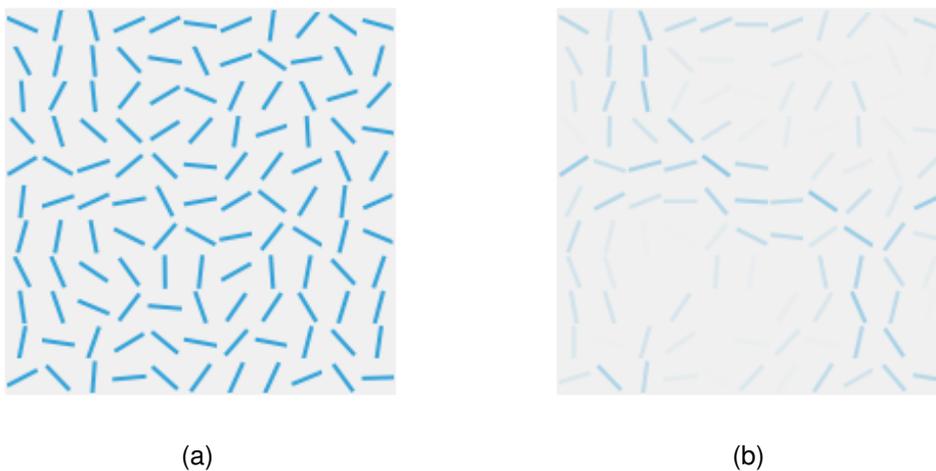
(a)   (b)

Figure 3.1: **Visualization of input and output of the model.** (a) Input of the model, a field of orientated bars. (b) Perceived bars. The more saturated the color, the stronger the response from the neurons for that particular bar. Some bars also may have different orientation from the input.

We have a stack of neurons tuned for different orientations for every location of the input (Fig.3.2). The perceived orientation is affected from two factors.

Every single location in our visual field has its own stack of neurons. The neurons from each stack are tuned for different orientations. They all spike with different intensities, depending on the bar presented. Their collective response, given by the population vector, forms the perceived orientation.

The complexity comes from the fact that neurons from one 'stack' are connected to neurons from other 'stacks'. Whenever a neuron spikes, he influences the neurons to which he is connected. Those connections and how they influence the perceived orientation in a dynamic setting is the main focus of our project.

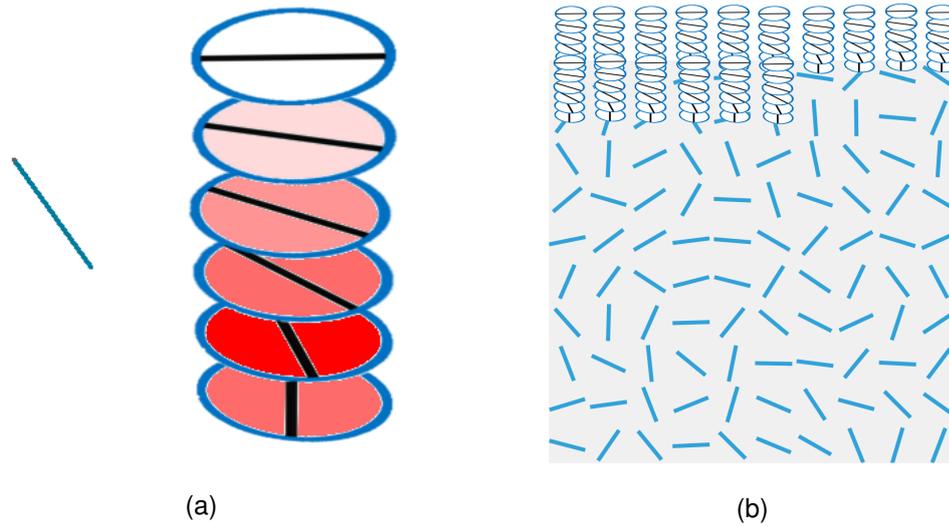(a)   (b)

Figure 3.2: **Visualization of the orientation selective neurons and their relationship with the presented input.** (A) Presented orientation(left) and responses of the orientation selective neurons(right). The more saturated the color, the stronger the response is. The neurons will spike with higher intensity, depending on the difference of the presented orientation and their preferred orientations. All the responses are combined, giving the final perceived orientation. (B) Schematic representation of the input and orientation selective neurons. Every orientation bar has its own stack of orientation selective neurons (only the first few are shown).

In order to perform our experiments we use a simple recurrent neural network. A recurrent neural network (RNN) is a type of neural network with two way connections between its neurons. Given a single neuron we calculate its response using Eq.3.1, where τ is a time constant, $\frac{dr(t)}{dt}$ is change of the firing of the neuron with respect to time, $r(t)$ is the firing rate of the neuron at time t, *in* is the input it receives (based the preferred orientation of the neuron, and the orientation of the bar presented) and *mod* is all the modulation from other neurons.

$$\tau\frac{dr(t)}{dt} = -r(t) + in + mod \tag{3.1}$$

We model the *in* according to the turning curve of a neuron(discussed in Sec.2.3), and the *mod* is calculated according to the law of smooth continuation, using the elastica principle (discussed in this section).

Eq.3.1 is central to the simulations ran in this report. Using this equation, we simulate a dynamic model of the orientation selective neurons in the primary cortex, and compare the results in relation to different visual illusions achieved in a static model [16].

We use the Euler's method [13] to solve Eq.3.1. We discretize the time and calculate the change of spiking of the neuron for every time step (Eq.3.2).

$$\frac{dr(t)}{dt} = \frac{-r(t) + in + mod}{\tau} \qquad (3.2)$$

An example simulation of one neuron with no modulation from other neurons and constant input $in = 1$ is shown in Fig.3.3.
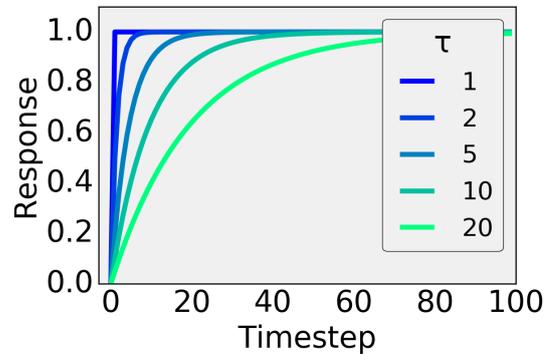

Figure 3.3: **Simulation of a neuron.**   In this example the neuron receives constant excitation (in) 1 and receives no modulation (mod). We plot the change of the response of the neuron as a function of time steps we take. We show the results for different values of the time constant τ. We see that the neuron eventually settles in a stable state.

3.2   Single bar

First we model the perception of a single bar. A stack of orientation selective neurons tuned for different orientation is responsible for perception of the bar presented.

(a)

(b)

Figure 3.4: **'Stack' of neurons for one location.** a) Visualization of neurons in a stack form b) Neurons in unrolled form. Both of the visualization are for purely illustrative purposes. Visualization a) is used to explain the general model, while visualization b) better explains the connections between the neurons.

As discussed in Sec.2.3 the activity of a neuron forms a bell shaped curve, depending on the stimulus presented (Fig.2.4). Given a certain neuron with preferred orientation ϕ_i and presented orientation θ_c, we modelled the activity by the von Mises equation (Eq.3.3).

$$g(\phi_i, \theta_c) = A_c exp(k_c cos2[\phi_i - \theta_c]) \tag{3.3}$$

The curve we get as a result (Fig.3.5) has similar shape as the one found to be in real neurons experimentally (Fig.2.4). The function $g(\phi_i, \theta_c)$ from Eq.3.3 is the central drive *in* from Eq.3.1.
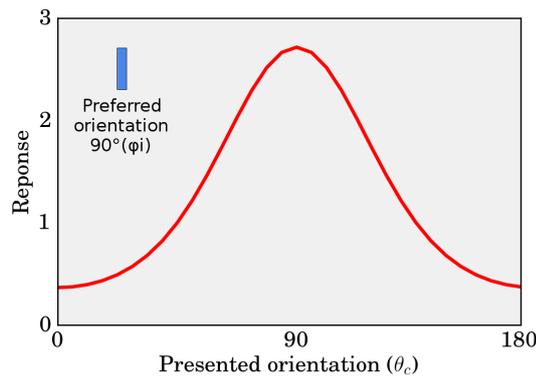

Figure 3.5: **Tuning curve.** Activity of a neuron with a preferred orientation $90°$ as a function of different presented orientations

To get a perception of the bar presented we combine the responses of all the neurons. As described in Sec.2.4, we represent those responses as vectors, with direction their preferred orientation and magnitude, the strength of the response with respect to the stimuli. Summing those vectors gives us the perceived orientation (Fig.3.6).

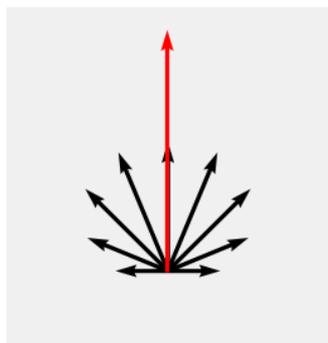Figure 3.6: **Population coding.** Population coding with 9 orientation selective neurons. The orientation presented is $90°$. As described in Sec.2.4 we represent the responses of the neurons as vectors and use vector addition to calculate the perceived orientation. The black vectors represent the responses of the 9 neurons, based on their tuning curves. The red vector represent the perceived orientation.

Since the preferred orientations are direction independent, they vary from 0 to π. As described in [16], to ensure circularity, we multiply all the responses by 2. Then we add them together and divide them by 2 at the end.

$$\vec{R}_{perceived} = \frac{1}{2}\sum_i 2\vec{r}_i \tag{3.4}$$

Finally we take the direction of $\vec{R}_{perceived}$ as the perceived orientation and the length, and the length as the magnitude of response.

3.3 Two bars

We extended the model so we can feed two orientations and have orientation selective neurons for both. We added recurrent connection between the neurons with the same preferred orientations, (Fig.3.7). This adds contextual modulation, as the perceived orientation of a single orientation in the visual field is influenced by the other one.
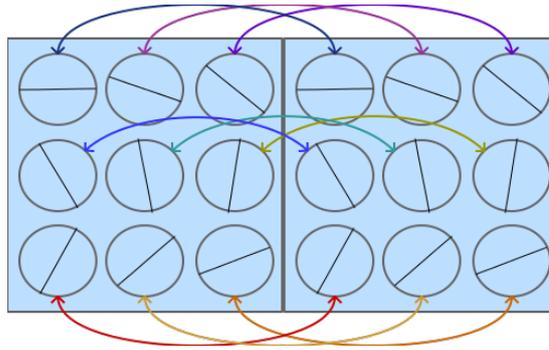

Figure 3.7: **Limited connectivity of orientation selective neurons for two bars.** In this iteration of the model we have neurons for detecting two bars. We add modulation between neurons with the same preferred orientation.

The firing rate of the pairs of same orientation selective neurons in the two visual fields is calculated from Eq.3.5 and Eq.3.6, where $[x]_+$ is rectification with $[x]_+ = x$ for $x > 0$ and $[x]_+ = 0$ for $x \leq 0$.

$$\tau\frac{dr_1(t)}{dt} = -r_1(t) + [in_1 + w_{12}r_2]_+ \tag{3.5}$$

$$\tau\frac{dr_2(t)}{dt} = -r_2(t) + [in_2 + w_{21}r_1]_+ \tag{3.6}$$

If we omit the rectification the linear equation can diverge. Non linearities are better to model biology, however they are also harder to analyze.

3.4 Multiple edges, limited connectivity

Next we extended the model, so we could have any number of stimuli (Fig.3.8). Every neuron (except the ones at the end at the visual field) is connected with the eight closest neurons, which have the same preferred orientation as his (Fig.3.8). We can extend the formulas 3.5 and 3.6 to:

$$\tau_{syn}\frac{dr_i(t)}{dt} = -r_i(t) + [in + \sum_j w_{ij}r_j]_+ \tag{3.7}$$
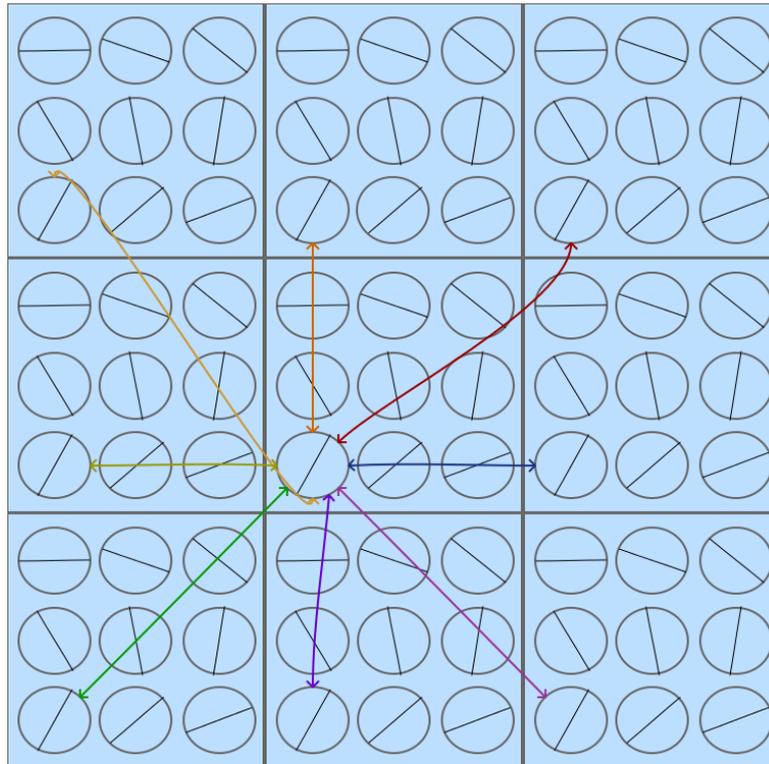

Figure 3.8: **Limited connectivity of orientation selective neurons for multiple bars.** We extend our model for an arbitrary number of stimuli. Again we add modulation only between neurons with the same preferred orientation. We connect every neuron with its 8 closest neighbours. (Connections for only one neuron are shown in the figure)

3.5 Multiple edges, full connectivity

The next modification we did was to add full connectivity between the neurons. We set the weights depending on the closeness of the neurons to each other and the similarity of their preferred orientation. To explain how we setup the weights, let use an example. Let's have a $10x10$ visual field with different orientations, as in Fig.3.1 and 9 orientations selective neurons. Unrolling the $10x10x9$ matrix, we have a vector of 900

neurons all together. We can setup $900x900$ weight matrix defining the all connections between the neurons.

We define the distance between every two neurons l and m in Eq.3.8, where i_l is the x position of neuron l in the weight matrix and j_l is the y position. Similarly for neuron m.

$$d_{l,m} = \sqrt{(i_l - i_m)^2 + (j_l - j_m)^2} \tag{3.8}$$

Next we have to define a quantitative measure of how similar two neurons are, based on their preferred orientation. The details of how we can do this using the elastica energy are described in Sec.3.6. For now we will just assume there exists a function $e_{l,m}$ defining how similar and strongly connected two neurons are, based on their orientation. The strength of the connection between every two neurons l and m is the same as the recurrent connection between l and m, so the matrix is symmetric with respect to the main diagonal. Thus we have Eq.3.9.

$$w_{l,m} = w_{l,m} = \frac{e_{l,m}}{d_{l,m}} \tag{3.9}$$

We can vectorize the updating of the network as in Eq.3.10, where W now is a weight matrix.

$$\tau \frac{d\vec{r}(t)}{dt} = -\vec{r}(t) + [\vec{in} + W\vec{r}]_+ \tag{3.10}$$

Finally we have to remove the modulation between neurons which have the same receptive field. Thus we have Eq.3.11, where I is the identity matrix.

$$\tau \frac{d\vec{r}(t)}{dt} = -\vec{r}(t) + [\vec{in} + (W - I)\vec{r}]_+ \tag{3.11}$$

3.6 Elastica energy

The final part is implementing the elastica energy [16] in our model (function $e_{l,m}$ from Sec.3.5). The elastica energy measures the total curvature between two bars and follows the laws of good continuation described in Sec.1. In our model we define the elastica energy as function measuring how strongly two orientation selective neurons should be connected. Based on neurons' preferred orientations and locations of the bars they are responsible for detecting, we calculate a number defining how strong the modulation between the neurons should be. Some examples of elastica curves with their respective energies are shown in Fig.3.9.
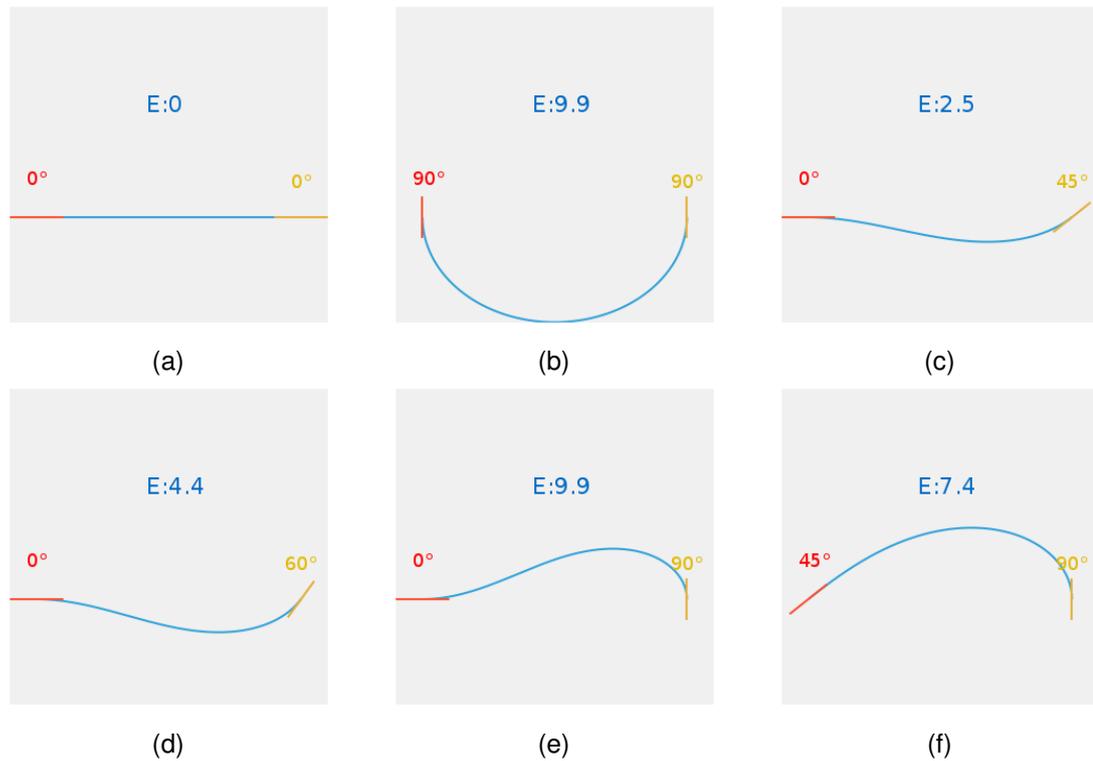
Figure 3.9: **Elastica energies.** Elastica energies for different bar configurations. The smoother the line connecting two bar, the smaller the energy. Two bars which lie on the same line have energy zero (a), while two vertical lines have very high elastica energy (b). More examples of elastica curves and their respective energies can be seen in (c), (d), (e) and (f). The elastica curve and energy are distance independent, hence the missing scales.

We will use the setup in Fig.3.10 to describe how we calculate the elastica modulation between different neurons.
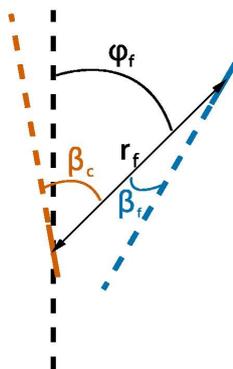

Figure 3.10: **Definition of angles between two bars.** Two bars and the corresponding angles between them, used in different formulas. We will refer to the orange bar as center and the blue line as flanker. We will refer to this figure to explain the elastica energy. (Figure taken from [16])

To find the elastica energy between the two bars, we have to measure the total curvature. One way to measure the total curvature is to integrate over the entire length of the curve and measure the relative angle at each position. However this method is computationally expensive. In this report we are going to use an approximation method used in [16], discovered by [24] and [19]. To calculate the approximation we use the existing code from [15].

We define θ_c as the orientation of the center, θ_f as the orientation of the flanker, ϕ_f as the angle between the flanker and a vertical bar, r_f as the distance between the center and flanker bar, $\beta_c = \phi_f - \theta_c$ and $\beta_f = \theta_f - \phi_f$. Then we have the elastica energy calculated according to Eq.3.12.

$$E(\theta_c, \theta_f, \phi_f) \approx 4(\beta_c^2 + \beta_f^2 - \beta_c \beta_f) \tag{3.12}$$

Next we calculate the modulation term for a given center and flanker bar, according to Eq.3.13. E_0 controls the excitation and inhibition ration of the modulation. r_f scales the modulation based on distance between the two bars. a is a constant modifying the strength of the modulation.

$$h_{add}(\phi_i, \theta_f, \varphi_f, r_f) = -\frac{a}{r_f}(E(\phi_i, \theta_f, \varphi_f) - E_0) \tag{3.13}$$

In our experiments we use an additive model, that is the modulation from nearby neurons is added to the response of the current neuron. In comparison in a multiplicative model we multiply the response of a neuron by all modulation terms. Since the static model described in [16] uses a multiplicative model, it is important to first distinguish the differences between the two different ways of applying modulation. Sec.5.4 goes in details showing that despite the different way of applying modulation they have similar effect.

Finally, Eq.3.14 shows the full equation of updating the response rate of a neuron.

$$\tau\frac{dr_i(t)}{dt} = -r_i(t) + [g_i + \sum_j h_{add}(\phi_i, \theta_f^j, \varphi_f^j, r_f^j)r_j(t)]^+ \tag{3.14}$$

In our experiments we use time constant $\tau = 6$. We take the positive value of $g_i + \sum_j h_{add}(\phi_i, \theta_f^j, \varphi_f^j, r_f^j)r_j(t)$ to prevent the response rate of a neuron below 0, which is impossible in a real neuron, indicated by $[]_+$.

Fig.3.11 gives further intuition about how the modulation between neurons works. In the first subfigure we visualise the full stack of orientation selective neurons for the left location and the orientation selective neuron for horizontal position for the right location. The blue connections between the neurons show how strongly connected they are, based on the elastica principle. The more saturated the colour the stronger connected they are. It's important to note that the strength of the connection is independent of the bars presented at the two locations.
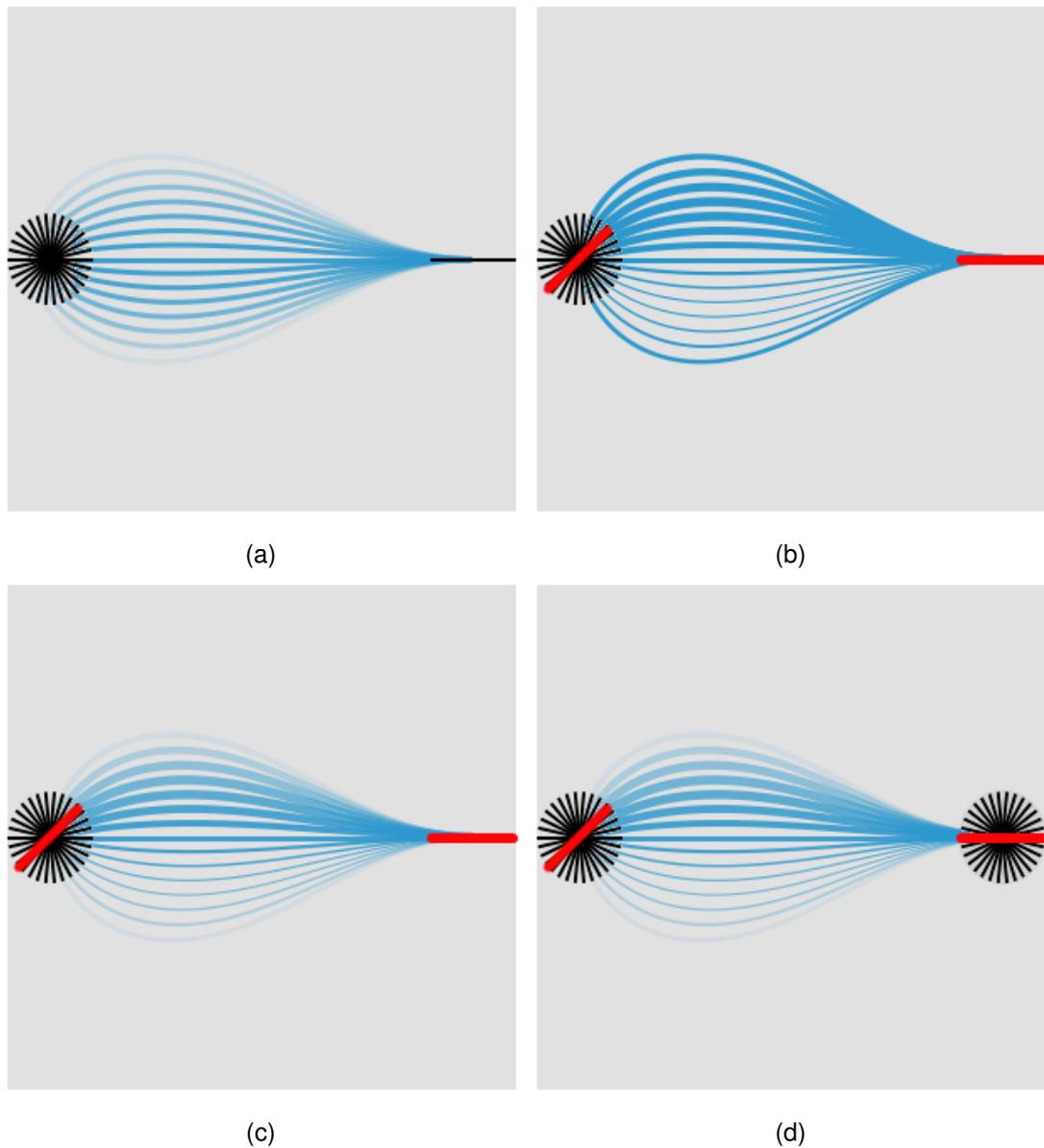
Figure 3.11: **Elastica principle, intuition for static and dynamic model** (a) Strength of the connection between a stack of neurons and nearby neuron tuned for horizontal position (the more saturated the color the stronger the connection) (b) Strength of the spiking of the stack when a bar is presented on the left (the thicker the bar, the stronger the spike) (c) Combined a and b (d) We have a stack of neurons for every bar in the model described here.

In subfigure (b) we add bar stimulus for each location (center on the left and flanker on the right). We focus our attention to the bar on the left with its stack of neurons. The thicker a blue curve is, the stronger the response of a neuron will be for the presented bar. This is defined by the already discussed von Mises function.

Subfigure (c) combines the two concepts. The more saturated the curve, the stronger the connection between two neurons. The thicker the curve, the stronger the response

rate of the neuron of the left. The plot gives us intuition which neurons influence each other the strongest, based on both the strength of the connection between them, but also their current firing rate.

Subfigures (a), (b) and (c) represent h_{add}, $r_j(t)$ and $h_{add}r_j(t)$ respectively in Eq.3.13.

Subfigure (d) illustrates the extension of our model in comparison to the model developed in [16]. Instead of calculating the modulation directly from the presented bar, all the flankers bars have their own stack of neurons from which we calculate the effect. Moreover we let the flankers receive modulation themselves and leave the whole system to interact with respect to time.

Chapter 4

Implementation

This section discusses the choice of programming languages and libraries, the benefits and challenges of using them and how they were addressed. During the implementation stages, we went through variety of changes, depending on the current stage of the project. First we implemented versions of visual fields, receptive fields, tuning curves and population coding. Next we implemented a model of the input the orientation selective neurons in the V1 cortex receive and modelled their behaviour. We gradually extended our model, to include more options for changing the connections between two neurons. We added an option to freely specify the position of the bars, instead of assuming fixed matrix grid. We use different tools for visualization and address some performance issues of simulating the model and running different experiments.

4.1   Initial choice of programming language

Our first choice of programming language was Matlab. Matlab is a high-level scripting language, highly optimised for linear algebra operations. It is a well suited language for the purposes as it takes a lot of the complexity of memory management, parameter passing, multiple memory spaces, etc, of language like C++ has for example. As matrices and vectors additions and multiplications were the main bottleneck in this project, Matlab provided the necessary performance, while being simple and convenient to use. Moreover as most of the functions in Matlab can receive as an input a single number, vector or matrix, the model we built can be easily extended and tested for different configurations. Their integrated IDE with interpreter, standard debugging tools (breakpoints, continue, step in/out, etc.), workspace of current variables in scope, provided additional convenience in the initial stage of development.

4.2   Model implementation

We implemented versions of visual stimuli the orientations selective neurons in V1 receive, tuning curves and population coding. The visual stimuli was implemented

as a field of different bars (or edges, lines) of particular orientation, so a matrix with numbers from 0 to π. As mentioned in the previous section most of the functions in Matlab accept numbers, vectors and matrices as their arguments. We take advantage of this, as we implement functions for one neuron and test them for expected output. Then the functions can be used for multiple neurons, when running more complicated experiments. We gradually extended the form on the input from a single orientation bar, to two and multiple ones in a form of matrix. We also extended the modulation connections between different neurons. Along different implementations we took advantage of the optimized linear operations in Matlab, and we keep our code vectorized, rather than using loops loops. The only exception is the simulation of different time steps of interactions between neurons, as the next state depends on the previous one.

4.3   Change of development tools

As the work progressed it became clear that Matlab, may not be the best choice of programming language for the project. After running some initial experiments, issues started coming up, which lead to transition to different set of programming tools, which we used for the final experiments. In our model we have different orientations bars, with a group of orientation selective neurons spiking for each bar and influencing the spiking of nearby neurons. It is a very high dimensional data, hard to visualize. Moreover as we have dynamic interactions implement by a recurrent neural network, we have the above mentioned data for every time step of our simulation. As the project grew bigger, some of the disadvantages of the weak code organization of Matlab became apparent, making hard to keep all the code base well structured.

After careful consideration we decided to rewrite the work we've done in Python taking advantage of libraries like Holoviews [26], Matplotlib [12] and Numpy. We also started using IPython notebooks [25]. Although the transition process took a couple of weeks, it yielded number of advantages outlined below.

Python

- Scalability - every function can be easily extended, by adding a new parameter and setting a default value, so it does not change the previous behaviour of the function

- Compatibility - Python is compatible with number of useful libraries, some of which used are described below

- Link to previous work - We took advantage of some of the code base of [16]. In particular we used the methods for calculating the elastica energy and visualizing the elastica curves.

Holoviews

- Interactive visualizations - building complex interactive visualization, with respect to any number of parameters. In case of our problem, we used it for visualization of perceived orientation with respect to time

Matplotlib

- Main tool for static plots - although Holoviews provides some really advanced plotting capabilities, its API is sometimes complicated and tedious to use. Matplotlib is much widely used libraries with rich documentations and examples online.

Numpy

- Numerical operations - Numpy provides number of mathematical operations as well as functions for matrices and vectors manipulation. In addition its syntax is almost identical to Matlab, speeding up the transition process.

IPython Notebook

- Reproducible research - experiments can be specified and ran in a notebook. Results are shown under every experiment, also giving the option to run part or all of them again.

- Documenting - support from markdown cells (in addition to the code cells for the experiments) with rich formatting, including support for LaTeX.

Using the above stack of software tools greatly improved not only the development process, but also conducting and documenting experiments.

4.4   Final model changes

After transitioning to Python we incorporated the elastica principle in our model. We also extended our model to custom positions of the neurons, rather than the fixed matrix grid. Instead of calculating the locations of the orientations, based on their position in the matrix, we can use a $1xN$ vector to represent all the neurons orientations together with $2xN$ matrix to represent their locations. This allowed us to reproduce most of the experiments in [16], in the dynamic setting of the model. For some of the bigger experiments we ran, we also implement circular connection between neurons (Fig.5.12). Fig.4.1 shows all the work done for the project.
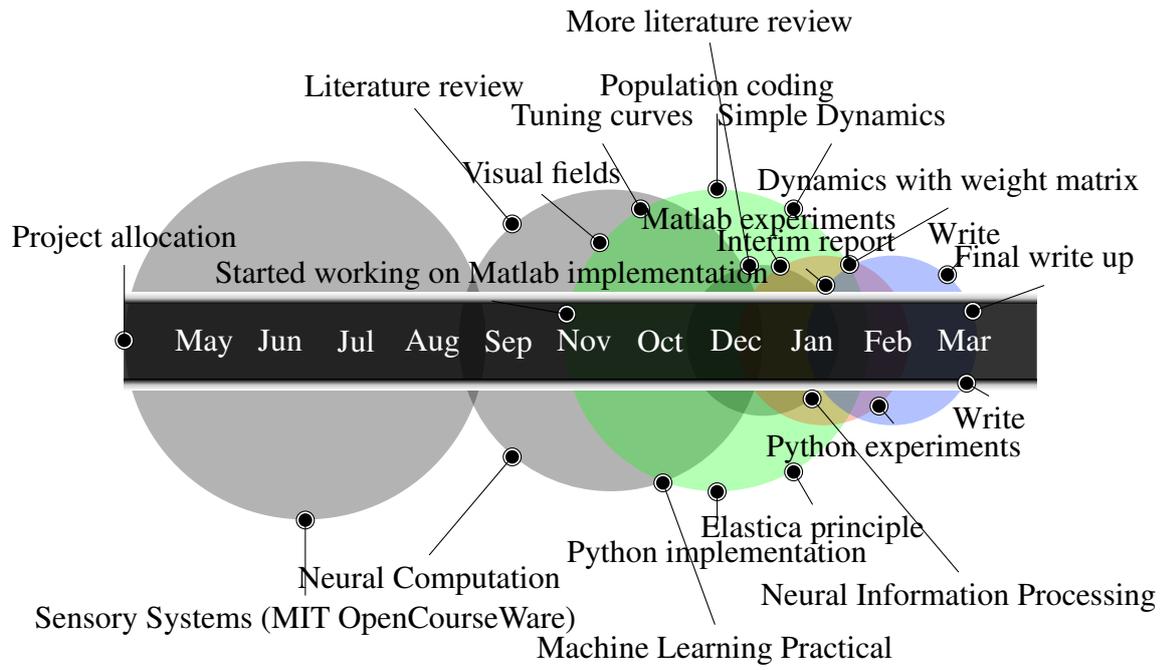
Figure 4.1: **Timeline of the project.** Research,Implementation,Experiments,Write up

Chapter 5

Experiments

In this section we test our model on variety of known visual effects - tilt illusions, pop out effect and contour extraction. We also reproduce some of the experiments from [16]. We discuss and compare the results from the two models. We explore the effect of different parameters and their relevance to the models. We also compare the results we obtain with collected biological data.

5.1   General discussion

Before running experiments for different visual effects, it is important to note the effect for different parameter values in our model. Although the additive model is not linear (Eq.3.14), the non linearity has little quantitative effect (Fig.5.14,e). The sum of the central drive and all modulation from nearby flankers, usually does not go below 0. For the purpose of exploring the behavior of the model for smaller set of varying parameters, we will assume a linear system.

The elastica modulation h_{add} has two free parameters, $E0$ (excitation/inhibition ratio) and a (strength of the modulation). As described in [16] $E0$ has no effect on the tilt illusions, pop out effects and contour extraction as we measure only relative changes in the response of the neurons.

The central drive of a neuron, modeled by the von Mises function (Eq.3.3), has two free parameters as well, k_c (width) and A_c (strength of the response). Similarly A_c has no effect on the effect on the experiments we perform (Fig.5.1).

Finally changing the number of orientation selective neurons per bar has no qualitative effect in our model. The number of neurons becomes relevant when we start adding noise to the central drive of the neurons [22]. In our experiments we will use population coding of 32 neurons.

The modulation between neurons depends on the strength constant a and distance r_f between them (Eq.3.13). They have the reciprocal effect. Increasing the distance r_f

between the neurons have the same effect as decreasing the strength constant a. We will use different values of r_f in our experiments.

To summarize, in this section we discussed the effects on different parameters of our model. We have shown why a lot of them don't have effect on the experiments we conduct. We will focus on how the distance between the presented stimuli (rf) and the width of the central drive (k_c) affect the experienced illusions.
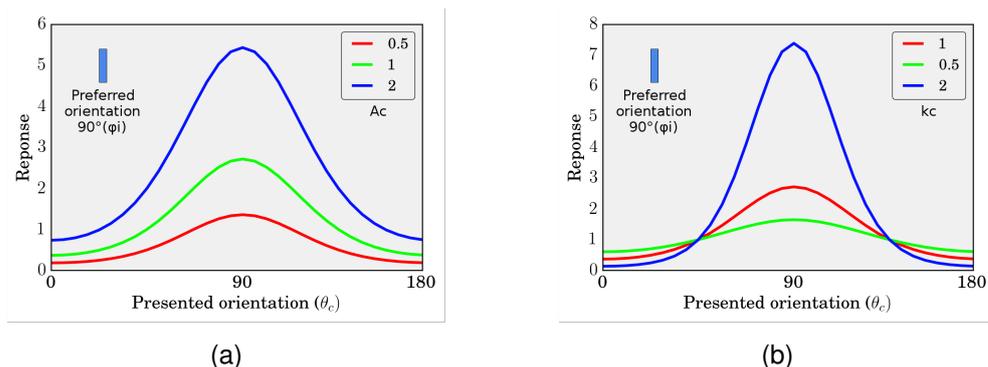

(a)   (b)

Figure 5.1: **Effect of A_c and k_c on the tuning curve of a neuron.** (a) A_c controls the strength of the response. (b) k_c controls the width. In exploring different visual effects caused from the modulation between neurons, we measure only relative changes. We can use any value for A_c, without loss of generality, as the number just specifies the strength of single neuron response. We use the same number for all neurons, so the relative differences remain the same. When $k_c = 1$, we get similar looking curve as in Fig.2.4. [16] again uses the same number, which helps comparing the results from this report and the results presented in the paper. In our experiments we use $A_c = 1$ and $k_c = 1$.

5.2 Tilt illusions

In this section we explore variety of tilt effects. In all of the experiments we have a similar setup of center bar and a number of flanker bars around it (Fig.5.2). We compare the results between our model, reproduced experiments from [16] (Fig.5) and biological data where possible. As in our model, the center bar influence back its flankers, we also show the modulation that the flankers experience.
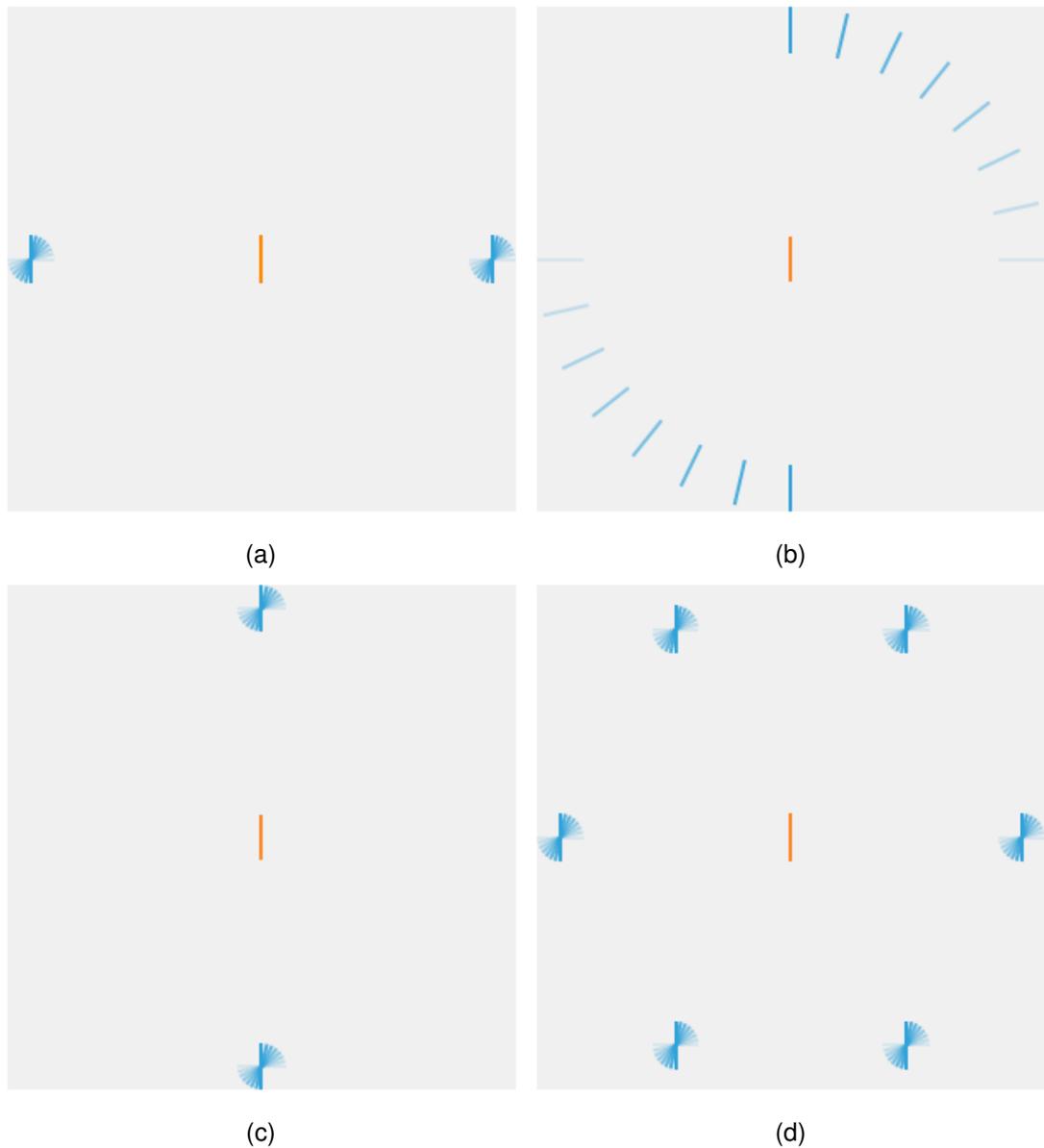
Figure 5.2: **Various tilt experiments.** The central bar (orange) stays fixed while we rotate and/or move the flankers (blue) around the center. We experiment with different number of flankers, vary their position and orientation around the center bar. a) Vary the orientations of two horizontal flankers. b) Rotate the two flankers around the center bar. c) Vary the orientation of two vertical flankers d) Vary the orientation of six flanker arranged in a hexagon shape around a center bar.

5.2.1 Tilt illusion 1

In this experiment we have a fixed center bar and two flankers, one on the left and one on the right of the center bar (Fig.5.2, a). We measure their effect on the center bar, as we vary their orientations. We compare our results with the data gathered from [14].

Visualizing the weight matrix of the strength of connections between different neurons

gives further intuition of modulation between different locations. The matrix specifies the connectivity between every orientation selective neuron tuned for different orientation ($0°$ to $180°$) and location (left flanker, center bar, right flanker). The connectivity can be seen in Fig.5.3.
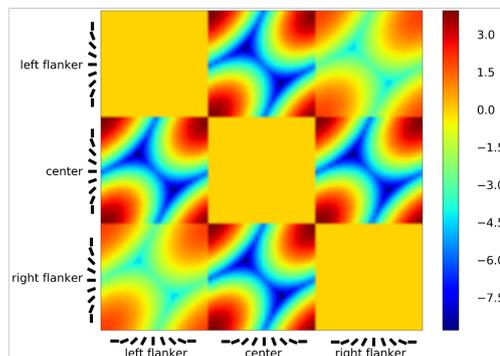

Figure 5.3: **Weight matrix for three stimuli in a line.** The matrix specifies the strength of the connections between every neuron. We note a couple of things. The matrix is symmetric with respect to the main diagonal, as we have symmetric connections between every two neurons (Eq.3.9). We don't have any connections between orientation selective neurons responsible for the same location. The two flankers are overall more weakly connected due to the bigger distance between them.

It is hard to make a side by side comparison between the models, due to different way they calculate modulation. In the passive model the modulation is directly calculated from the orientations of the flankers. In the dynamic model we calculate the modulation through the orientation selective neurons of the flankers. Thus we can't set the same value for the strength of those connections. We approach the problem by tuning the strength of the modulation for two models, until we get similar effects. Then we quantitatively vary r_f and we compare the results. In this particular experiment we use $a = 0.1$ for the static model and $a = \dfrac{0.1}{16}$ for the dynamic one.

We vary the orientations of the two flankers (the two of them always keep the same orientation, we vary them simultaneously). We plot the results as a function of different flanker orientations. We run multiple experiments for different distances between the bars, changing the the r_f in Eq.3.14. The results can be seen in Fig.5.4.
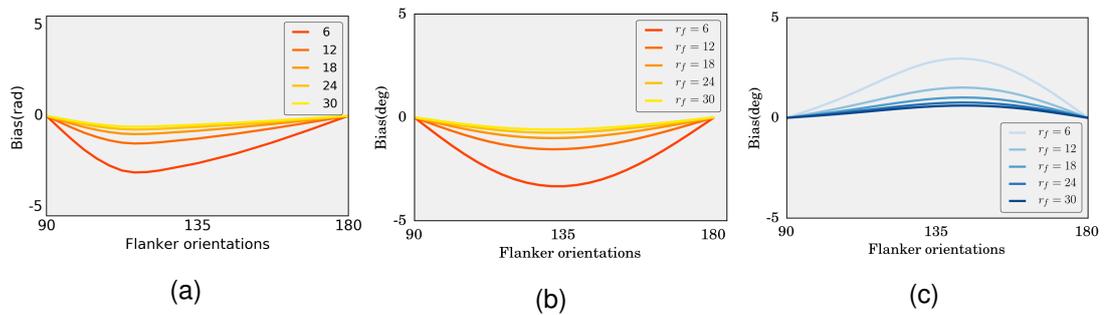
Figure 5.4: **Experienced tilt illusions for different flanker orientations, tilt illusion 1.** Experiments setup is illustrated in fig.5.2 a) (a) Tilt illusion of the center bar in a static model (b) Tilt illusion of the center bar in a dynamic model. (c) Tilt illusion of the flanker bars in a dynamic model. The two flankers have the same modulation, because the elastica energy is direction independent.

The dynamic model we described here, changes with respect to time. What we have shown is the stable state that the system eventually settle into (after 50 time steps). Since we have full connectivity we can also see the experienced effect in the flankers, hence the extra sub plot for the dynamic model. Since our model is direction independent, the two flankers experience the same effect.

The effect on the center bar in our model is repulsive as in the static model [16] and biological data from similar experiment done with monkeys [14]. However we note that the curve is shifted to the right, with the strongest repulsive effect happening when the flankers have orientations just below $135°$, rather than earlier as suggested by both [16] and [14]. We also notice the attractive effect on both of the flankers.

It is useful to also explore the dynamics of the system, how the response of the neurons vary with respect to time. In Fig.5.5 we show the change of the orientation selective neurons for center bar, magnitude of the overall activity and change in orientation with respect to time. We notice the gradual change of the magnitude of the neurons' responses, as well as the gradual shift in their response, based on nearby modulation.
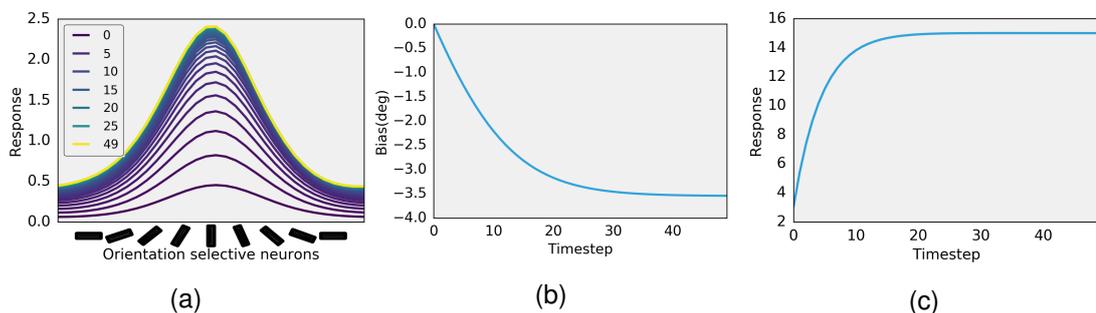

Figure 5.5: **Change in perceived orientation and magnitude of the response, with respect to time.** (For this particular experiment both flankers have orientation $135°$, $r_f = 6$) (a) Population coding of the center bar for different time steps. (b) Change in perceived orientation. (c) Change in the magnitude of the response.

5.2.2   Tilt illusion 2

In this experiment vary the orientations of the flankers as in previous experiment, but at the same time we vary their position as well (Fig.5.2,b). Again we plot the tilt effects in the two models (Fig.5.6).

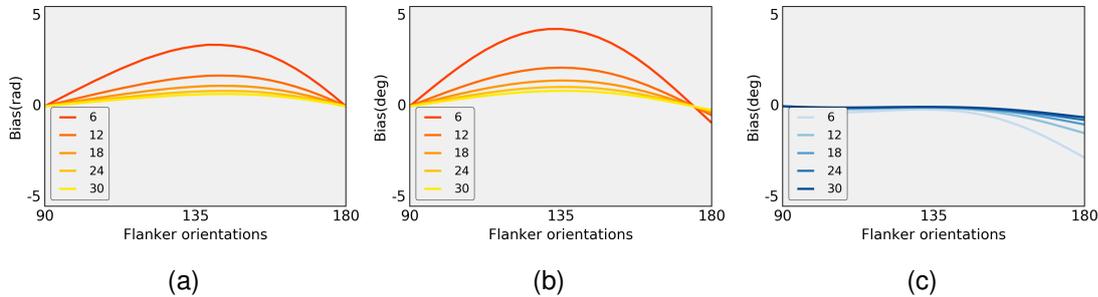(a)   (b)   (c)

Figure 5.6: **Experienced tilt illusions for different flanker orientations, tilt illusion 2.**   Experiments setup is illustrated in fig.5.2 b) (a) Tilt illusion of the center bar in a static model (b) Tilt illusion of the center bar in a dynamic model. (c) Tilt illusion of the flanker bars in a dynamic model.

The effect on the center bar is predominantly attractive as in [16]. In a static the center bar does not receive any modulation, as the flankers cancel each other's effect. However in a dynamic model, we also have recurrent modulation back to the flankers. We note the strong repulsive modulation on the flankers bars when they are horizontal. The change in their orientation could have sub sequentially led the repulsive effect on the flanker bar.

5.2.3   Tilt illusion 3

In this experiment the flanker bars are on a vertical line together with the center bar (Fig.5.2,c). We show the results in Fig.5.7.
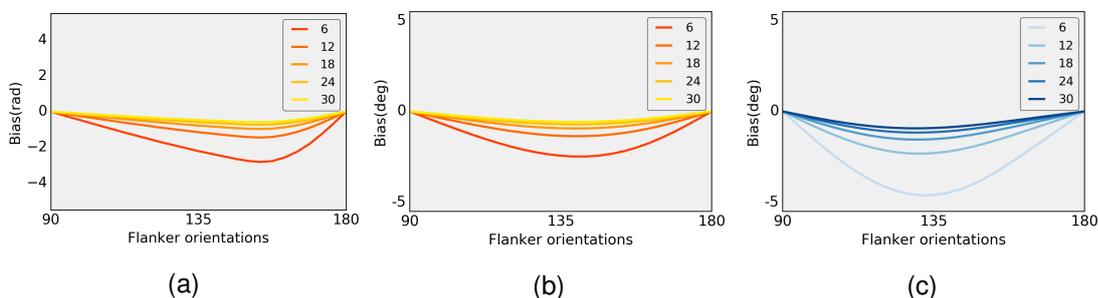

(a)   (b)   (c)

Figure 5.7: **Experienced tilt illusions for different flanker orientations, tilt illusion 3.**   Experiments setup is illustrated in fig.5.2 c) (a) Tilt illusion of the center bar in a static model (b) Tilt illusion of the center bar in a dynamic model. (c) Tilt illusion of the flanker bars in a dynamic model.

The effect on the center bar is repulsive as in the static model, however the strongest effect is again experienced for different flanker orientations. In contrast to the first illusion, this time the effect on the flankers is attractive.

5.2.4 Tilt illusion 4

In this experiment we have six flanker bars, instead of two as in previous experiments. The flankers are in hexagon around the center bar (Fig.5.2,d). The tilt effect on the center bar is shown in Fig.5.8 and tilt effect on the flanker bars in Fig.5.9.
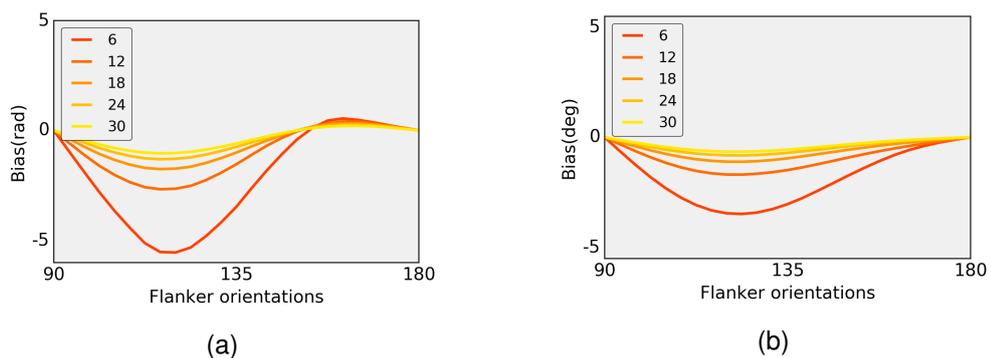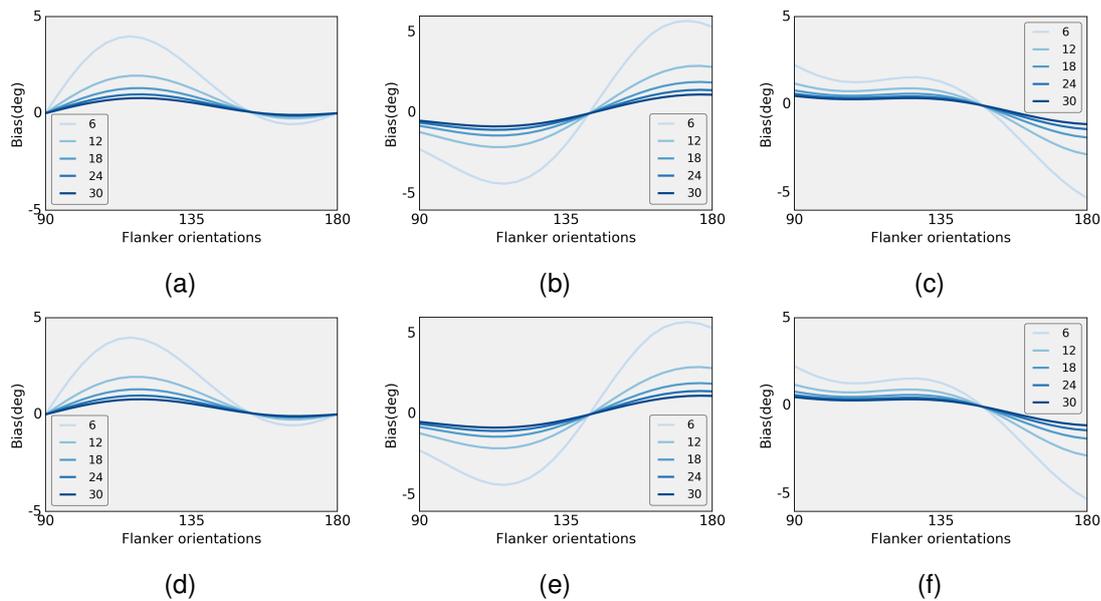

(a)   (b)

Figure 5.8: **Experienced tilt illusions for different flanker orientations, center bar, tilt illusion 4** (a) Tilt illusion of the center bar for different flaker orientations. The experiment reproduced is from [16], Fig.5, F (b) Tilt illusion of the center bar for different flanker orientations, in the dynamic mode. (c) Tilt illusion of the flanker bars for different flanker orientations, in a dynamic model

Figure 5.9: **Experienced tilt illusions for different flanker orientations, flanker bars, tilt illusion 4** Here we show the tilt effect on the six flankers. We start with plotting the change in the flanker on the most left (a) and plotting the rest of them moving clockwise (b,c..). Every two opposite flankers experience the same modulation as in previous experiments, hence the symmetry between figures a-d,b-e and c-f.

We compare the two models to the experimental data gathered from [29], where four people were observing the same experiment. In this experiment our model arguably performs better that a static model. If we average the tilt illusions observed by two four people, then the static model clearly explains the data. However if we look closely at the data from [29], we see that the data from three of the people closely matches the data from our model. At the same time the tilt effects experienced by the fourth person, significantly differ from the rest.
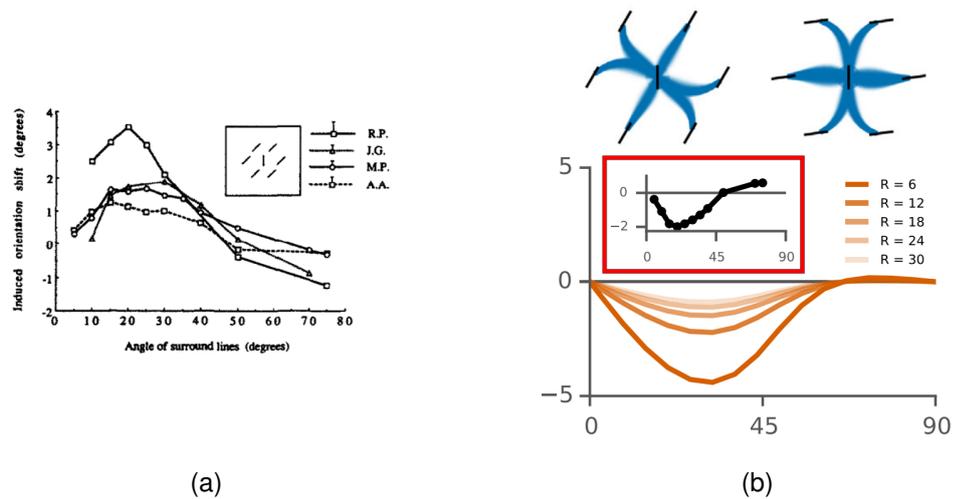
Figure 5.10: **Experimental data for the hexagon illusion.** (a) Experimental data from four people (R.P., J.G, M.P. and A.A) observing the hexagon illusion (the y axis is swapped) [29]. (b) Average of the data (in the red box) In this just averaging the response does not represent the data very well. J.G, M.P. and A.A experience consistent tilt effect for different flanker orientations. However we see that the perception of R.P. is a lot different from the rest of the three people. If we exclude R.P. from the data, then the dynamic model described in this report matches the data better. (figures taken from [29] [16])

As the experiments get bigger we can see more complex tilt illusions that happen, especially to the flankers. The tilt effect on two flankers, which lie on the horizontal with center, remains mostly attractive as Fig.5.4, c. However maximum strength of the effect is shifted when the orientation of the flankers are between $90°$ and $135°$.

5.3 Pop out effects and contour extraction

In this section we focus our attention on larger scale experiments. In the experiments performed in this section we also measure the strength of the overall response of group of neurons for a specific location. We use the saliency effect described in [21]. The saliency of a bar is its maximum response divided by the maximum response in the image. We find that similarly to [16] the dynamic model explains pop out effects and contour extraction. We visualize the output of our model with respect to time, showing dynamically how the detections happen (see Appendix). In the initial experiments we notice some unexpected results (Fig.5.11). However after some adjustment of the weights to ensure more even modulation (Fig.5.12) the results we get align with [21].
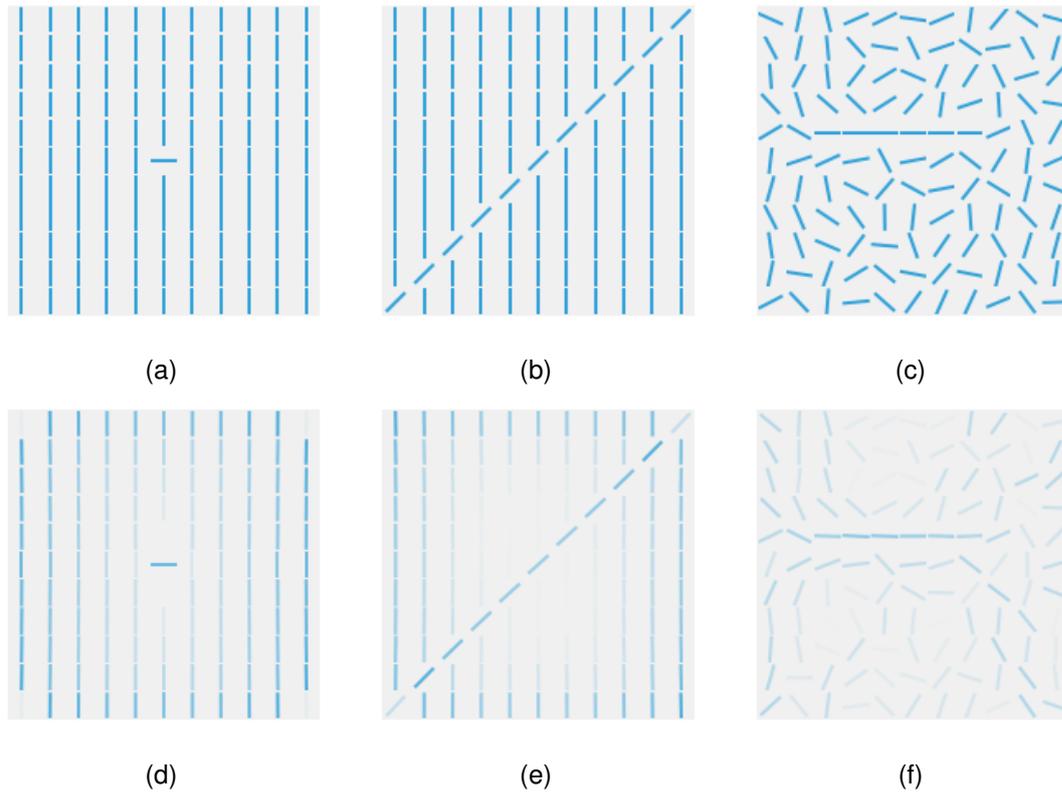
Figure 5.11: **Pop out and contour extraction with uneven modulation.** The first row represents the presented stimuli. The second one represents the perceived orientations. We notice the change in activity as we go from the edge stimuli locations to the center ones. The reason for this is the uneven modulation between different neurons. Neurons close to the edge of the visual field receive less modulation as they are further away from other neurons.
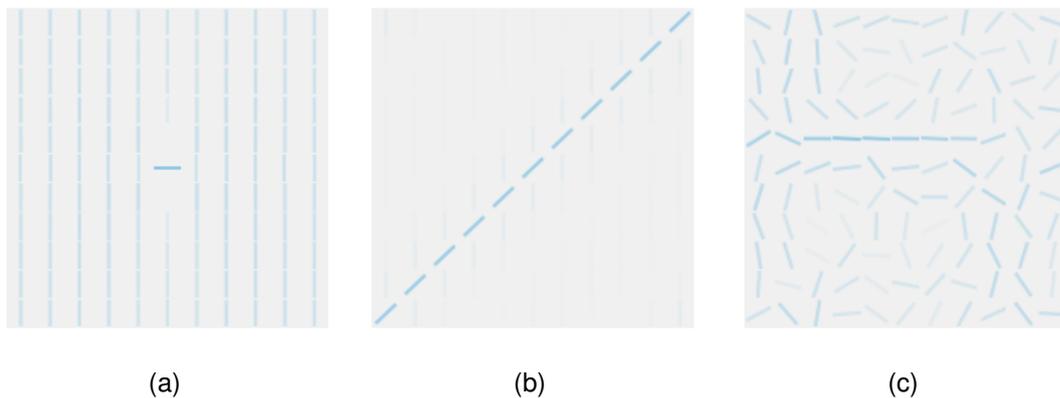

Figure 5.12: **Pop out and contour extraction with even modulation.** Here we show the output when we have even modulation independent of the position of the neurons on the visual field. We put the visual stimuli on a torus. (Given two neurons with difference between their coordinates i and j, visual field with size mxn, we define the distance r_f between the neurons as $r_f = min(distance(i,j), distance(i \pm m, j \pm n))$)

5.4 Additive and Multiplicative rules

In this section we compare two models of applying modulation from nearby neurons. Using additive rule, we add all the modulation terms to the central drive of the neuron as seen in Eq.3.13 and Eq.3.14.

Using multiplicative rule, we multiply the central drive by all modulation terms as seen in Eq.5.1 and Eq.5.2.

$$h_{mul}(\phi_i, \theta_f, \varphi_f, r_f) = exp[-\frac{a}{r_f}(E(\phi_i, \theta_f, \varphi_f) - E_0)] \tag{5.1}$$

$$\tau\frac{dr_i(t)}{dt} = -r_i(t) + g_i \prod_j h_{mul}(\phi_i, \theta_f^j, \varphi_f^j, r_f^j) r_j(t-1) \tag{5.2}$$

It is important to analyze the differences between the two as this report implements the additive rule and we compare our results with [16], which uses multiplicative rule. We use the setup shown in Fig.5.13 to compare the two models. We have a center bar (on the left), which orientation is encoded by number of orientation selective neurons. We also have a flanker bar (on the right) which affects the center bar. In this experiment we calculate the modulation between the flanker and center bar, directly rather than using neurons for the flanker bar as well. We also don't use a dynamic model.
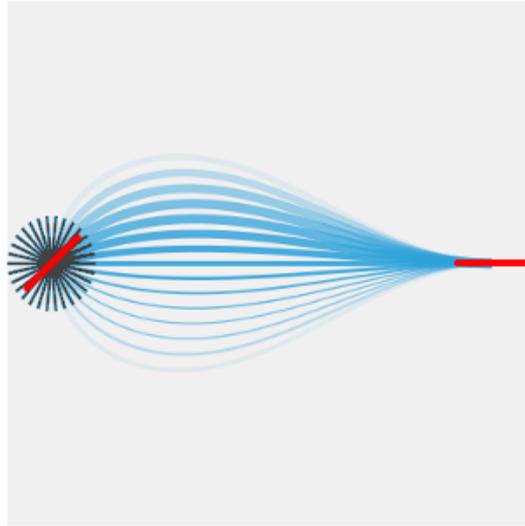

Figure 5.13: **Experiment setup.** Left red bar - center, right red bar - flanker, black bars - orientation selective neurons, blue curves - elastica curves. The position of the center bar is encoded by n orientation selective neurons. The modulation from the flanker is directly calculated from the orientation of the flanker bar, rather than through encoding it with orientation selective neurons. The more saturated the color, the stronger the connection between the orientation selective neuron and the flanker (not dependant on the presented center orientation). The wider the curve, the stronger the response of that neuron (dependent on the presented center orientation).

Fig.5.14 shows the different steps of calculating the modulation for the additive and multiplicative rules. We notice that the final curves of neural activity look quite different. However we also notice that the shift in response overall is similar - the curve has shifted up and to the left. The population coding of the neurons actually will show similar tilt in the perceived orientation.
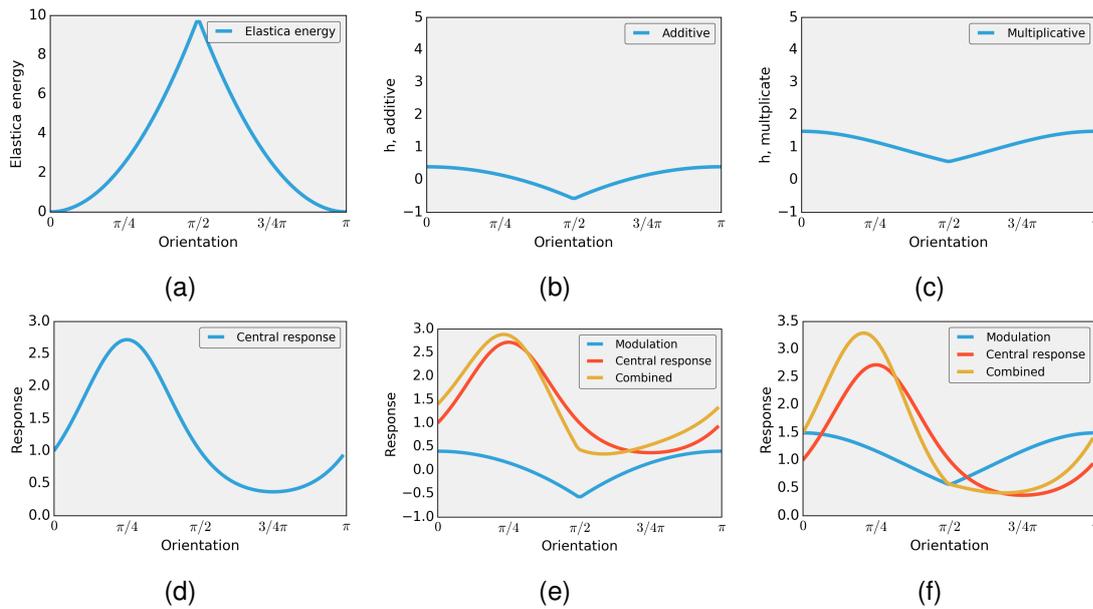

Figure 5.14: **Additive and Multiplicative model** (center bar orientation is $\frac{\pi}{4}$, flanker bar orientation is $\frac{\pi}{2}$) (a) Elastica energy (b) h, additive (c) h, multiplicative (d) Central drive (e) Final response for additive model (f) Final response for multiplicative model

Finally to measure the differences between the two rules as we vary the orientation of the flanker bar. We record the change in the perceived orientation after we do population coding, compared to the presented one. The results are summarized in Fig.5.15.
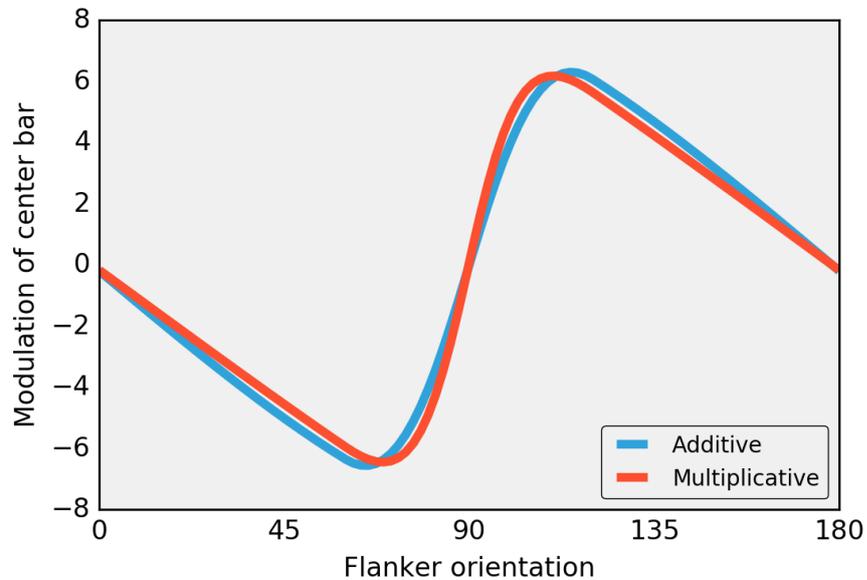
Figure 5.15: **Additive vs Multiplicative rules for different flanker orientations.** (center bar orientation is $\frac{\pi}{4}$) Although the tilt effects happen at different orientations and the strength of modulation is different, the change in the effect as we vary the flanker orientation is similar.

The models (at least in a static model) are not so different. This helped us compare the dynamic and static models. We opted to use the additive rule, as it is easier to be implemented efficiently in a dynamic model. However the combined responses, of the central drive and modulation, still look quite differently. The two rules had almost the same effect in a static model. However as we use orientation selective neurons for every bar, and let the neurons interact dynamically, the difference in the shifted tuning curves, could lead to significant changes.

Chapter 6

Evaluation

In this section we evaluate the results from the experiments we've run. We critically evaluate the performance of the dynamic model described in this report. We test our model on known visual illusions and effects and compare in with the static model developed in [16].

6.1 Tilt illusions

Our model showed similar tilt illusion compared to both the static model in [16] an different biological data [14] [29]. In the tilt illusion described in Sec.5.2.4 our model arguably performed better.

6.2 Pop out effects and tilt illusion

Our model of primary visual cortex also successfully describes pop out effects and contour extraction. We test on three stimuli and all of them behave as expected [21].

6.3 Additive and Multiplicative rules

We compare the ways of applying modulation between neurons. In in Sec.5.4 we show the similarity between the two rules. However in performing the experiment we used only two bar stimuli and we calculated the modulation only once. We didn't used orientation selective neurons for the flanker bar, but rather calculated the modulation directly. Even though the effect in our comparison looked similar (Fig.5.15), the experiments we ran were a lot different than how we compared the two rules. Moreover as we use a recurrent neural network, all the small changes between neurons' connections could lead to big shift in perceived orientation.

6.4   Modulation between neurons

We saw in Sec.5.3 that limited modulation on the edges of visual stimuli can lead to strange behaviour of the perceived tilt or pop out effects. Using circular connections in the bigger experiments (Sec.5.3) mitigated the problem. However this is something that remained unexplored in the tilt illusions. We can perform experiments with two variations of the weight matrix. We can ignore the feedback connections from the center bar back to the flankers, as well as the connections between the flankers themselves. In the second variation, we can model the connections as in Sec.5.3. For example the matrix from 5.2.1 can be modified as in Fig.6.1.

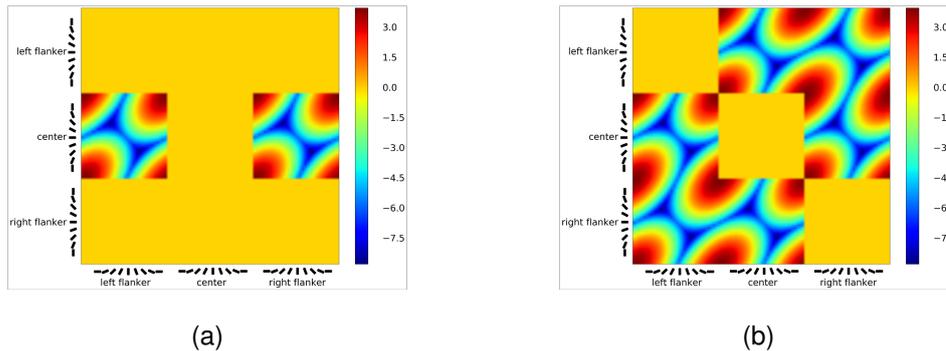| (a) | (b) |

Figure 6.1: **Variations of the weight matrix** (a) No recurrent connections back to the flankers (b) Assuming the distance between any two bars is the same

By using the weight matrix from Fig.6.1,a we can have modulation only from the flankers to the center bar as in [16]. However we are applying the modulation from orientation selective neurons, rather than directly from the presented bars. In this way we can analyse the importance and potential difference between calculating modulation directly and through set of neurons, without adding the complexity of recurrent connections.

6.5   Noise

We didn't add any noise to the spiking of the orientation selective neurons. This could leave to different effects, especially when the neurons are connected in a recurrent neural network. When we add noise, number of orientation selective neurons per bar starts to matter more as there is a relationship between the noise level, number of orientation selective neurons and the accuracy of the perceived response.

Chapter 7

Conclusion

In this report we implemented a dynamic model of the primary visual cortex. We modeled the connections between different orientation selective neurons, based on the elastica principle. We extended an already existing passive phenomenological model of the primary visual cortex. Our main contribution consisted of two parts. We modeled the modulation between different bars using neurons, rather than calculating the modulation directly from the present bars. We also added full connectivity between the neurons, with feedback connections. We tested our model on multiple visual effects - tilt illusions, pop out effects and contour extraction. We compared our model to the static and we found that we get similar results in many regards. Our model matches biological data collected from different experiments. In some cases it arguably matches the data better than the static model. We show that using elastica for modulation between neurons explains various observed effects not only in a phenomenological model, but in a biologically plausible dynamic system. This suggests that the elastica may indeed be one of the main principles in our primary visual cortex.

Bibliography

[1] Bagrat Amirikian and Apostolos P Georgopulos. Directional tuning profiles of motor cortical cells. *Neuroscience research*, 36(1):73–79, 2000.

[2] Bruno B Averbeck, Peter E Latham, and Alexandre Pouget. Neural correlations, population coding and computation. *Nature Reviews Neuroscience*, 7(5):358–366, 2006.

[3] Matthew J Baggott, Jennifer D Siegrist, Gantt P Galloway, Lynn C Robertson, Jeremy R Coyle, and John E Mendelson. Investigating the mechanisms of hallucinogen-induced visions using 3, 4-methylenedioxyamphetamine (mda): A randomized controlled trial in humans. *PloS one*, 5(12):1–13, 2010.

[4] James R Cavanaugh, Wyeth Bair, and J Anthony Movshon. Nature and interaction of signals from the receptive field center and surround in macaque v1 neurons. *Journal of neurophysiology*, 88(5):2530–2546, 2002.

[5] Vision computation from neurons to perception. Retinotopic Mapping. `http://fourier.eng.hmc.edu/e180/lectures/v1/node3.html`, 2016. [Online; accessed 21-January-2016].

[6] Gregory C DeAngelis, Izumi Ohzawa, and Ralph D Freeman. Receptive-field dynamics in the central visual pathways. *Trends in neurosciences*, 18(10):451–458, 1995.

[7] David J Field, Anthony Hayes, and Robert F Hess. Contour integration by the human visual system: evidence for a local association field. *Vision research*, 33(2):173–193, 1993.

[8] Apostolos P Georgopoulos, Ronald E Kettner, and Andrew B Schwartz. Primate motor cortex and free arm movements to visual targets in three-dimensional space. ii. coding of the direction of movement by a neuronal population. *The Journal of Neuroscience*, 8(8):2928–2937, 1988.

[9] Apostolos P Georgopoulos, Andrew B Schwartz, and Ronald E Kettner. Neuronal population coding of movement direction. *Science*, 233(4771):1416–1419, 1986.

[10] H. K. Hartline. The effects of spatial summation in the retina on the excitation of the fibers of the optic nerve. *American Journal of Physiology – Legacy Content*, 130(4):700–711, 1940.

[11] David H Hubel and Torsten N Wiesel. Receptive fields and functional architecture of monkey striate cortex. *The Journal of physiology*, 195(1):215–243, 1968.

[12] John D Hunter et al. Matplotlib: A 2d graphics environment. *Computing in science and engineering*, 9(3):90–95, 2007.

[13] Martin Hutzenthaler, Arnulf Jentzen, and Peter E Kloeden. Strong and weak divergence in finite time of euler's method for stochastic differential equations with non-globally lipschitz continuous coefficients. In *Proceedings of the Royal Society of London A: Mathematical, Physical and Engineering Sciences*, volume 467, pages 1563–1576. The Royal Society, 2011.

[14] Mitesh K Kapadia, Gerald Westheimer, and Charles D Gilbert. Spatial distribution of contextual interactions in primary visual cortex and in visual perception. *Journal of neurophysiology*, 84(4):2048–2062, 2000.

[15] Sander Keemink. Elastica code. `https://github.com/swkeemink/elastica`, 2016. [Online; accessed 22-March-2016].

[16] Sander W Keemink and Mark CW van Rossum. A unified account of tilt illusions, association fields, and contour detection based on elastica. *Vision research*, 2015.

[17] Emily Knight, Arthur Shapiro, and Zhong-Lin Lu. Drastically different percepts of five illusions in foveal and peripheral vision reveal their differences in representing visual phase. *Journal of Vision*, 8(6):967–967, 2008.

[18] Alfred Kobsa. Gestalt laws. `https://www.ics.uci.edu/~kobsa/courses/ICS104/course-notes/gestalt-continuity2.png`, 2016. [Online; accessed 29-March-2016].

[19] Thomas Leung and Jitendra Malik. Contour continuity in region based image segmentation. In *Computer VisionECCV'98*, pages 544–559. Springer, 1998.

[20] Raph Levien. The elastica: a mathematical history. *Electrical Engineering and Computer Sciences University of California at Berkeley*, 2008.

[21] Zhaoping Li. Contextual influences in v1 as a basis for pop out and asymmetry in visual search. *Proceedings of the National Academy of Sciences*, 96(18):10530–10535, 1999.

[22] Rodrigo Quian Quiroga and Stefano Panzeri. Extracting information from neuronal populations: information theory and decoding approaches. *Nature Reviews Neuroscience*, 10(3):173–185, 2009.

[23] Ashish Ranpura. Overview of Receptive Fields. `http://brainconnection.brainhq.com/2004/03/06/overview-of-receptive-fields/`, 2016. [Online; accessed 19-January-2016].

[24] Eitan Sharon, Achi Brandt, and Ronen Basri. Completion energies and scale. *Pattern Analysis and Machine Intelligence, IEEE Transactions on*, 22(10):1117–1131, 2000.

[25] Helen Shen et al. Interactive notebooks: Sharing the code. *Nature*, 515(7525):151–152, 2014.

[26] Jean-Luc R Stevens, Philipp Rudiger, and James A Bednar. Holoviews: Building complex visualizations easily for reproducible science. 2010.

[27] Alastair Townsend. On the spline. `http://www.alatown.com/spline/`, 2016. [Online; accessed 29-March-2016].

[28] unknown. the idea of fields. `http://crowwithnomouth.com/2014/11/18/the-idea-of-fields/`, 2016. [Online; accessed 29-March-2016].

[29] Gerald Westhhmer. Simultaneous orientation contrast for lines in the human fovea. *Vision research*, 30(11):1913–1921, 1990.

[30] Robert Andrew Wilson and Frank C Keil. *The MIT encyclopedia of the cognitive sciences*. MIT press, 2001.

Chapter 8

Appendix

8.1   Experimental data from Sec.5.3

Here we experiment with different stimuli and different strength of the modulation. For every experiment we plot a number of different time steps.
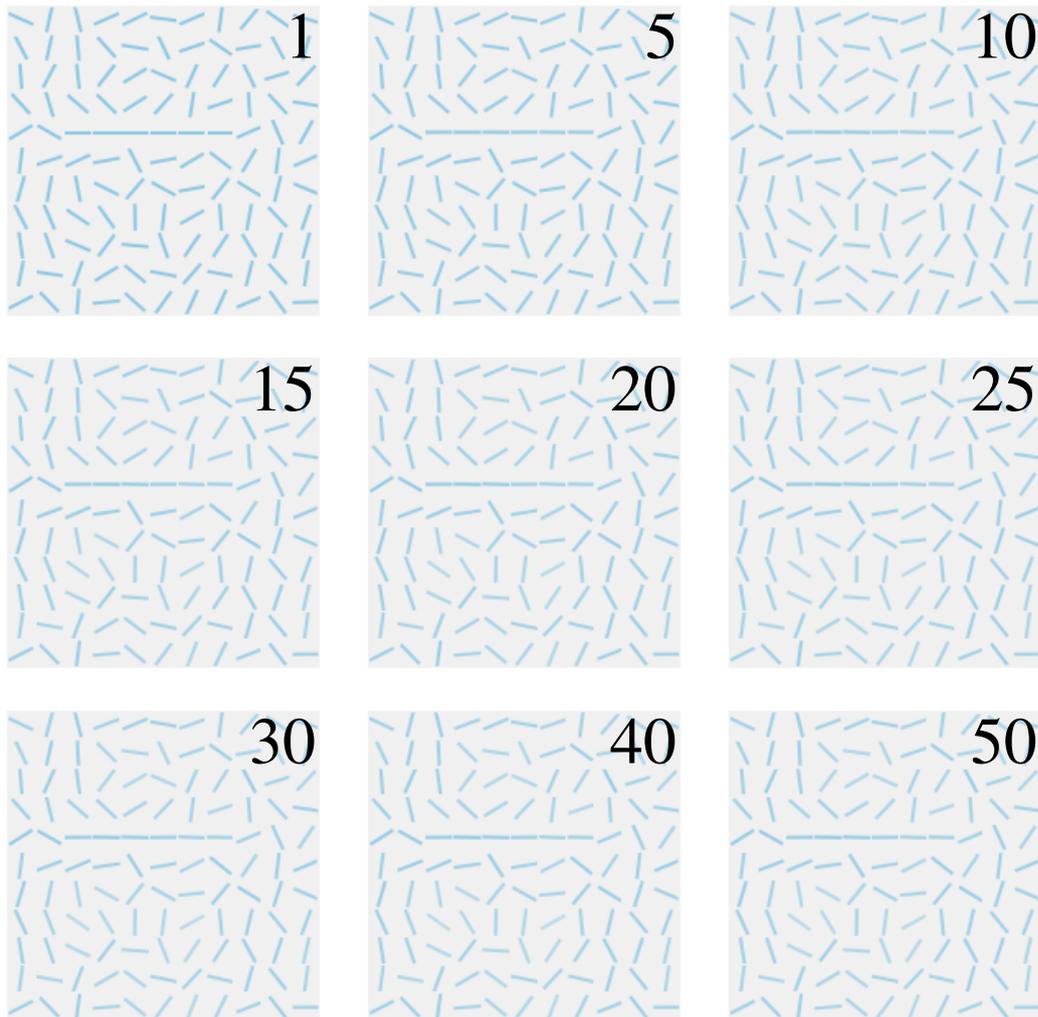
Figure 8.1: **Modulation strength - 0.001, contour**
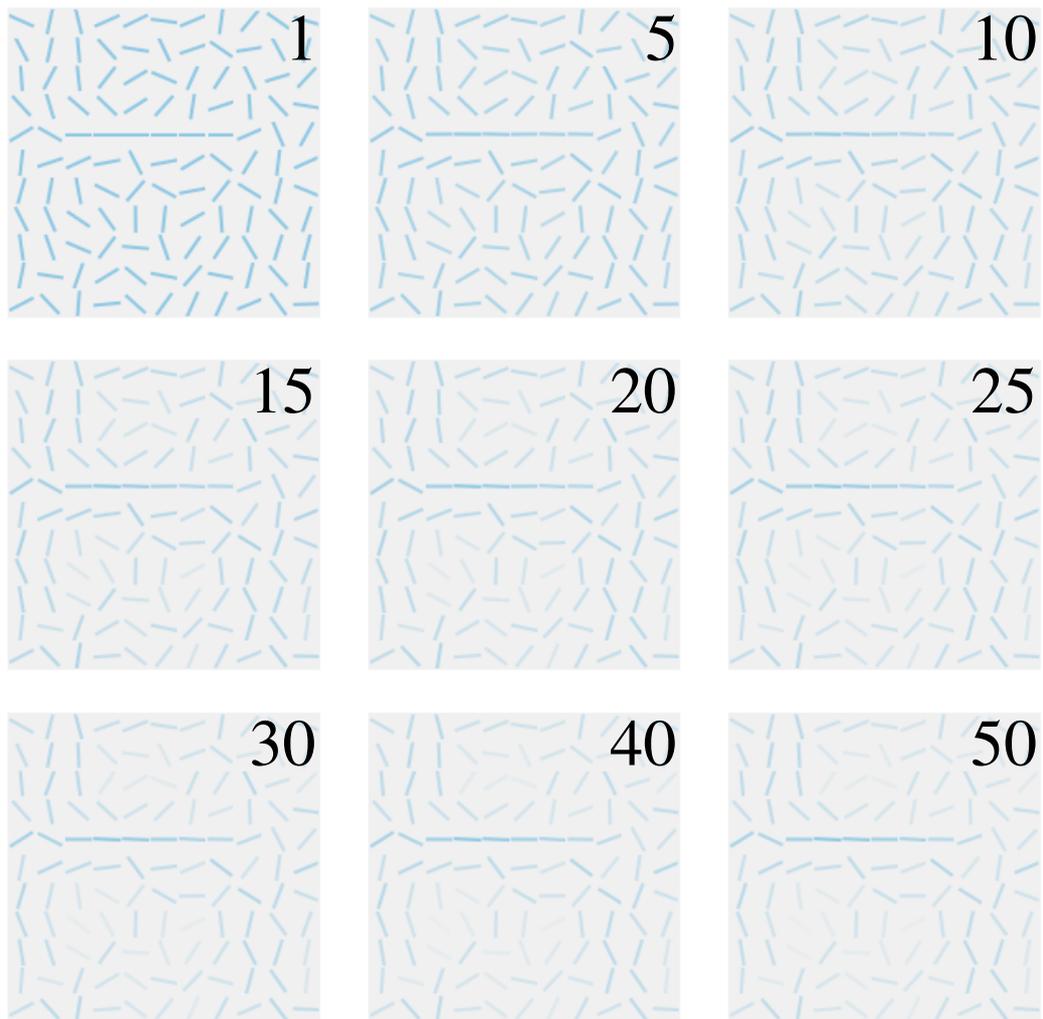
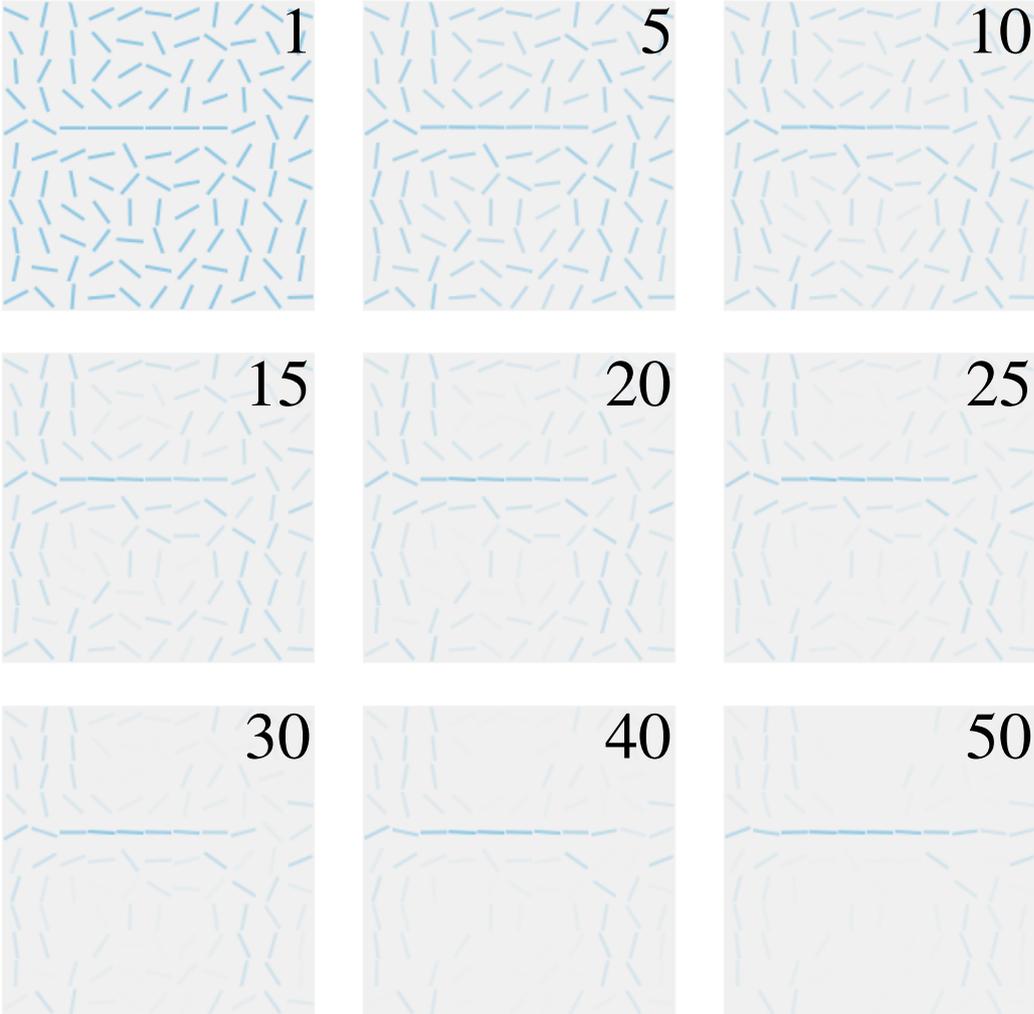Figure 8.2: **Modulation strength - 0.003, contour**

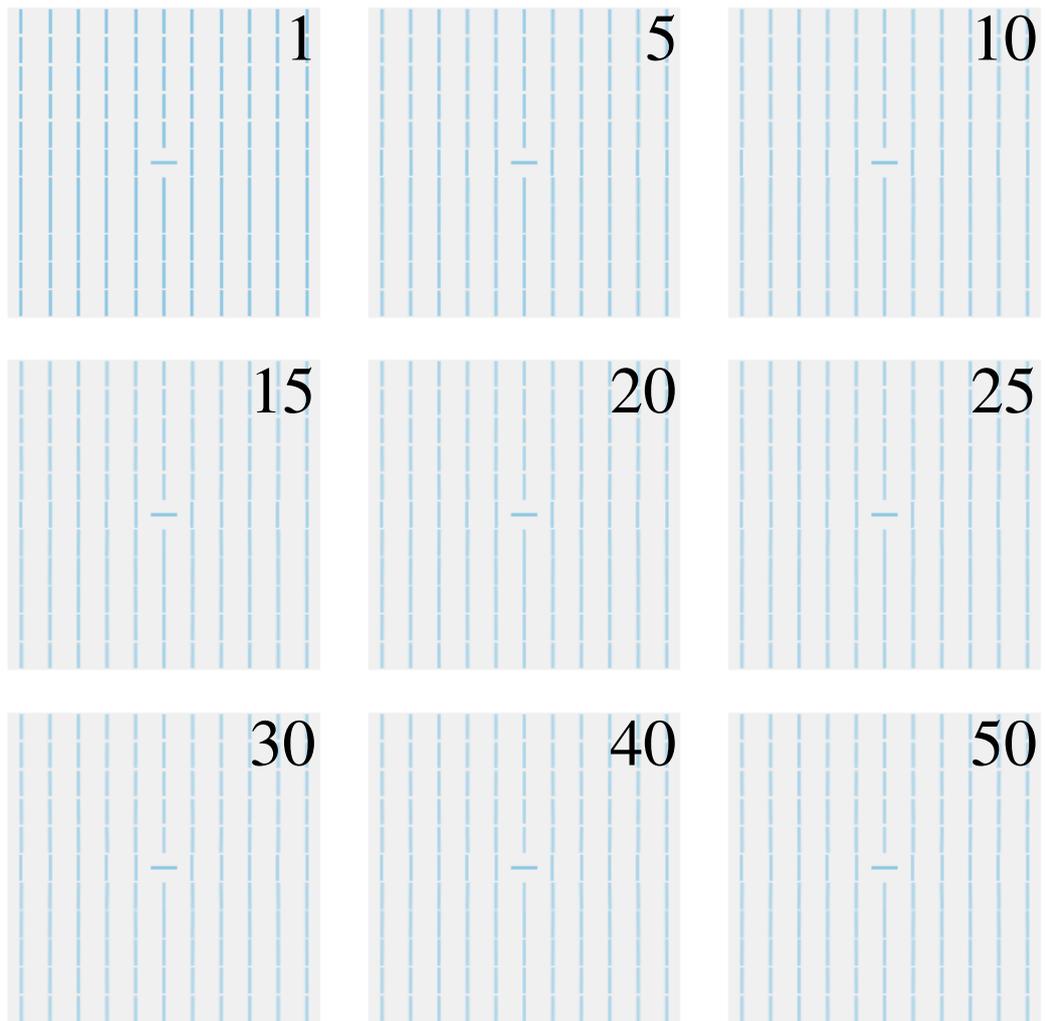Figure 8.3: **Modulation strength - 0.005, contour**
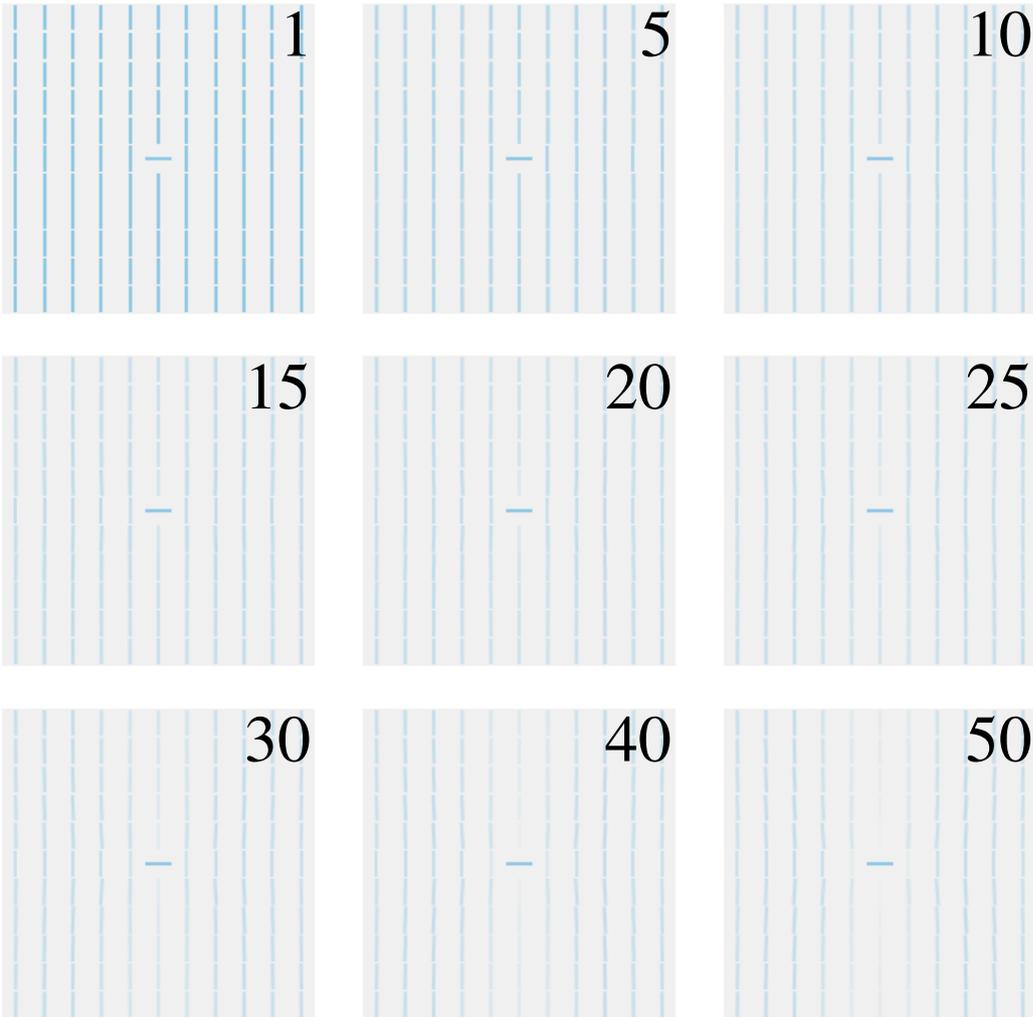
Figure 8.4: **Modulation strength - 0.001, bar**
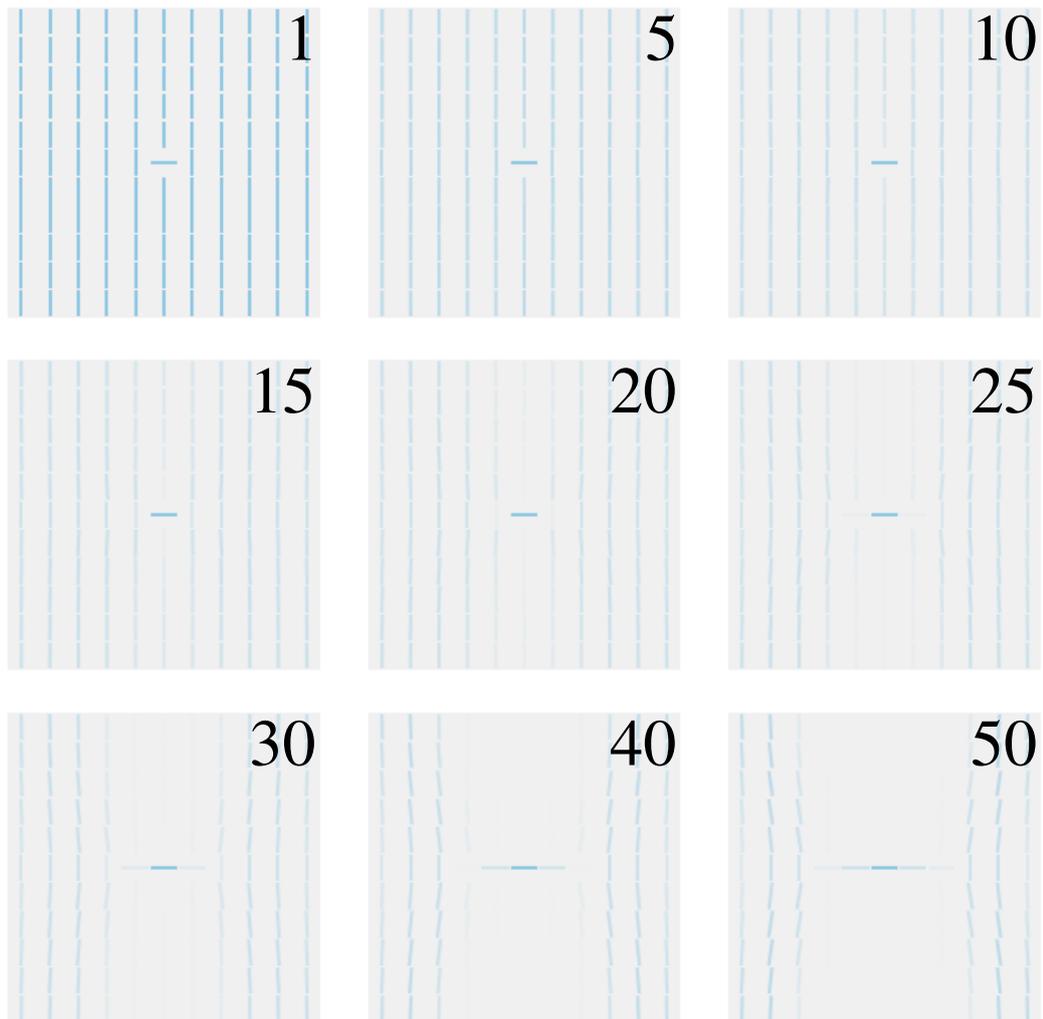
Figure 8.5: **Modulation strength - 0.003, bar**
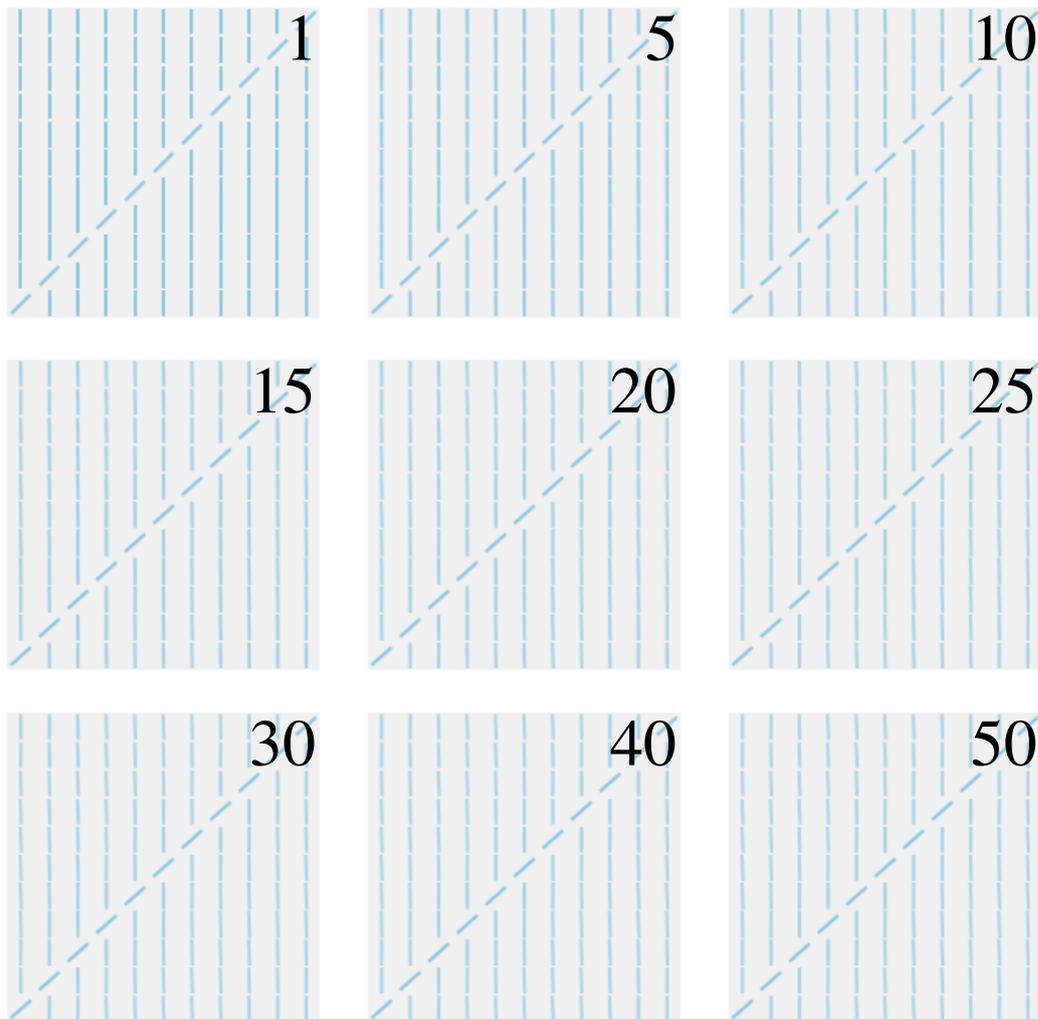
Figure 8.6: **Modulation strength - 0.005, bar**

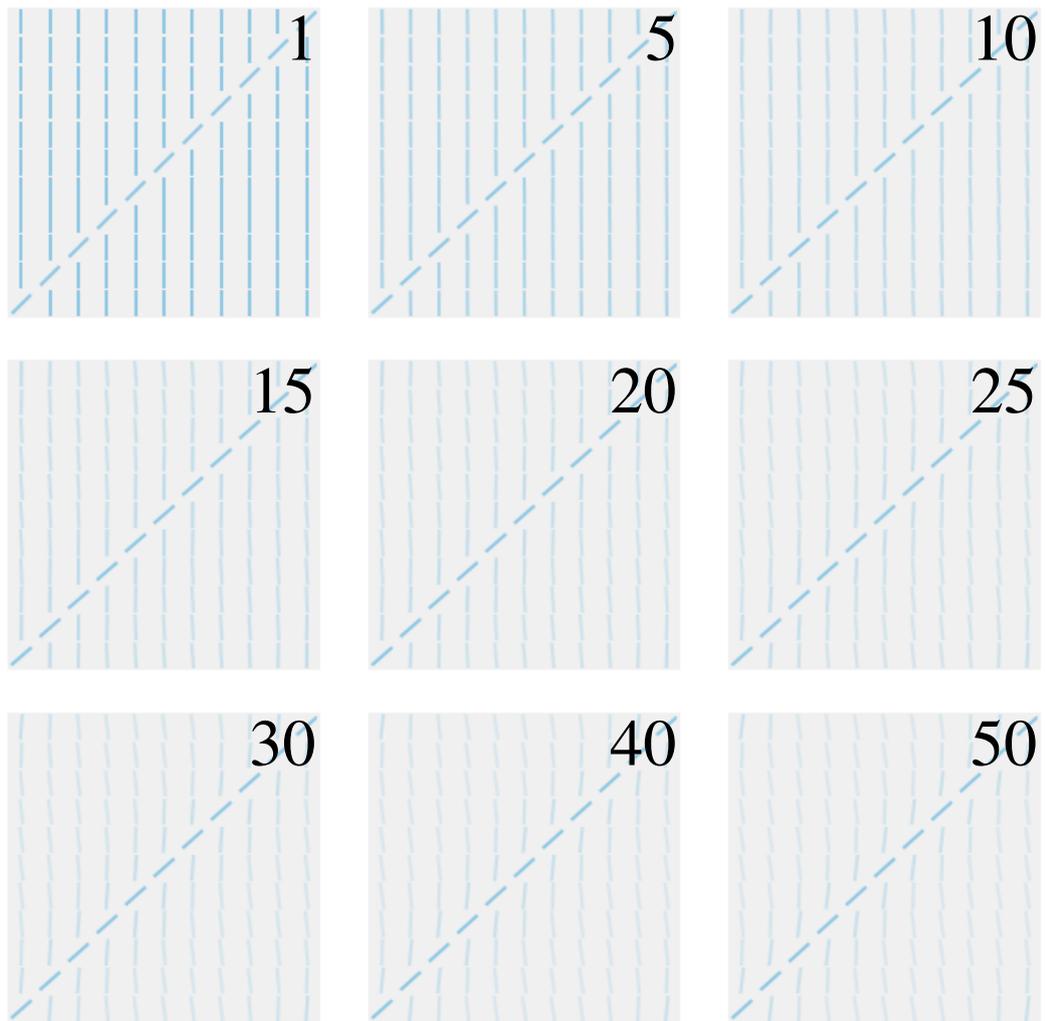Figure 8.7: **Modulation strength - 0.001, line**
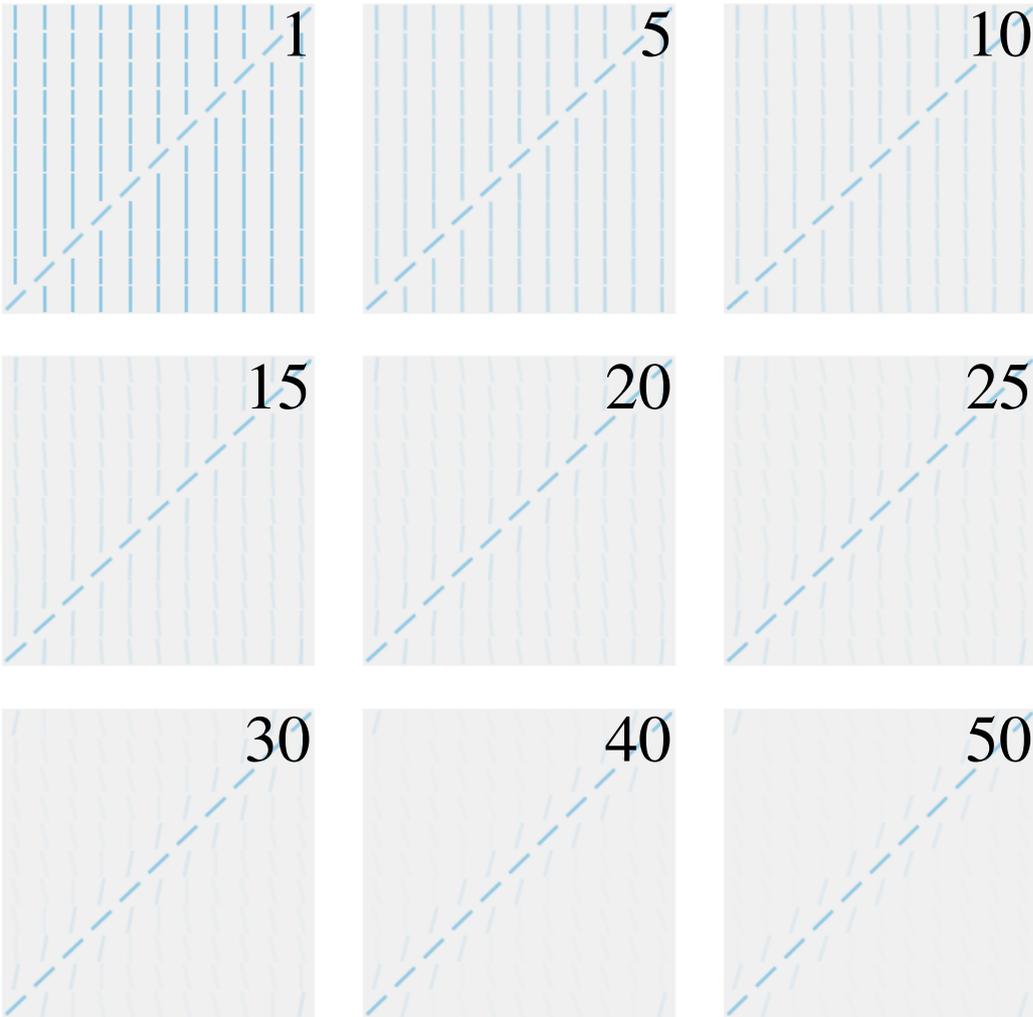
Figure 8.8: **Modulation strength - 0.003, line**

Figure 8.9: **Modulation strength - 0.005, line**